



**Georgia DOT Research Project**

**Sensing System Development for HOV/HOT (High  
Occupancy Vehicle) Lane Monitoring**

**Office of Materials and Research**

**Research and Development Branch**



GDOT Research Project No. RP 07-26

Sensing System Development for HOV (High Occupancy Vehicle) Lane Monitoring

Draft Final Report

SENSING SYSTEM DEVELOPMENT FOR HOV (HIGH OCCUPANCY VEHICLE) LANE

MONITORING

By

Wayne Daley  
Principal Research Engineer

Omar Arif  
John Stewart  
Jack Wood  
Colin Usher  
Erin Hanson  
John Turgeson  
Doug Britton

Georgia Tech Research Institute

Contract with

Georgia Department of Transportation  
In cooperation with  
U.S. Department of Transportation  
Federal Highway Administration

February, 2011

The contents of this report reflect the views of the author(s) who is (are) responsible for the facts and the accuracy of the data presented herein. The contents do not necessarily reflect the official views or policies of the Georgia Department of Transportation or of the Federal Highway Administration. This report does not constitute a standard, specification, or regulation.

## **ACKNOWLEDGEMENTS**

We would like to acknowledge the assistance of GDOT personnel at the TMC, GDOT Research, Randy Guenzler and Michael Hunter faculty of the school of CEE at Georgia Tech.

## **ABSTRACT**

With continued interest in the efficient use of roadways the ability to monitor the use of HOV/HOT lanes is essential for management, planning and operation. A system to reliably monitor these lanes on a continuous basis and provide usage statistics would be very helpful in supporting management operations and decision making. In this study we evaluated the potential of an imaging system that would be installed on the median wall of HOV/HOT lanes to acquire data on the vehicles using the lanes and the occupancy of these vehicles. A lab prototype consisting of an IR illuminator, a camera, vehicle trigger, a computer and software to control the system was integrated and evaluated. Data was taken at GTRI facilities, sites on the Georgia Tech campus and also on interstate 85. The images taken were then analyzed for their ability to provide the information needed on the usage of the lanes. The results indicate that it would be possible to build a system that would be able to provide the data needed to support the operation of HOV/HOT lanes.

**Key words:** HOV, HOV lanes, HOT lanes, traffic, vehicle occupancy, machine vision, computer vision

## TABLE OF CONTENTS

ACKNOWLEDGEMENTS.....	i
ABSTRACT.....	ii
TABLE OF CONTENTS.....	iv
LIST OF FIGURES.....	vi
INTRODUCTION.....	1
PROCEDURE .....	10
FINDINGS.....	11
SENSING.....	11
Geometry.....	11
Trigger Selection .....	13
Imaging.....	15
Window/Glass Studies .....	15
Camera Selection .....	17
Optics and Illumination .....	19
Incident Angles.....	23
PROCESSING ASPECTS.....	26
CONTROL SYSTEM SOFTWARE .....	28

IMAGE PROCESSING SOFTWARE .....	30
SYSTEM TESTING.....	31
Street Testing .....	31
Interstate Testing.....	33
Distance and Illumination Tests.....	34
Illumination Pattern Evaluation .....	34
Working Distance Tests.....	38
PROCESSING/ANALYSIS.....	41
CONCEPT FOR DEMONSTRATION FIELD INSTALLATION.....	44
Hardware .....	45
Software.....	46
RECOMMENDATIONS .....	46
REFERENCES .....	48
BIBLIOGRAPHY .....	49
APPENDICES .....	50
Appendix I: Sample Output Images .....	50
Appendix II: Software Design.....	52
Appendix III: Image Processing Approaches.....	63
Appendix IV: LED Evaluation.....	81



## LIST OF FIGURES

Figure 1: Passenger in Vehicle. ....	4
Figure 2: Extracted Passenger in Vehicle. ....	4
Figure 3: Transmission Properties of Infrared-blocking Automobile Glass. ....	6
Figure 4 Overhead view of Potential site using Google Sketch Up .....	12
Figure 5 Example view angle providing view of rear seat .....	12
Figure 6 Potential test site for demo system.....	13
Figure 7 Design for Glass Transmission Measurement System .....	16
Figure 8 Comparison of transmission measurement apparatus with CARY spectrophotometer.....	16
Figure 9 Transmission data from samples of commercially available windshields.....	17
Figure 10 Spectral response of the monochrome Chameleon camera.....	18
Figure 11 Perkin Elmer MVS 5770 IR Illuminator spectral output.....	20
Figure 12 Perkin Elmer MVS 5770 IR Illuminator power output vs. range.....	21
Figure 13 Sample Illumination LED array .....	23
Figure 14 Test apparatus for LEDs .....	23
Figure 15 Transmission measurements at various orientations.....	24
Figure 16 Effect of pitch on transmission .....	25
Figure 17 Effect of yaw on transmission.....	25
Figure 18 Initial System configuration IR illuminator t a laser trigger and camera. ....	26
Figure 19 System undergoing initial testing .....	27

Figure 20 GTRI Sample vehicle.....	27
Figure 21 Sample output image.....	28
Figure 22 second sample image.....	28
Figure 23 Graphical User Interface to control the system.....	30
Figure 24 Graphical User Interface for file viewing .....	30
Figure 25 Georgia Tech Test Site .....	31
Figure 26 Interstate-85 Test Site.....	31
Figure 27 Campus Sample 1.....	32
Figure 28 Campus Sample 2.....	32
Figure 29 First I 85 Sample 1.....	33
Figure 30 First I 85 Sample 2.....	33
Figure 31 First I 85 Sample 3.....	33
Figure 32 First I 85 Sample 4.....	33
Figure 33 Nine feet from wall, No fresnel.....	37
Figure 34 – Nine feet from wall, Fresnel with grooves out (the prescribed usage orientation).....	37
Figure 35 – Nine feet from wall, Fresnel with grooves in.....	38
Figure 36 Reflected Energy at Different Distances.....	39
Figure 37 Falloff in reflected energy intensity vs. distance .....	40
Figure 38 Second I 85 Sample 1 .....	41
Figure 39 Second I 85 Sample 2 .....	41

Figure 40 Sample processed output green region window red region people .....	44
Figure 41 Concept for demo system implementation .....	46
Figure 42 - Software Design Block Diagram.....	56
Figure 43 - DoProcess Function Flowchart .....	59
Figure 44 - Program Dialog with Camera Option.....	60
Figure 45 - Program Dialog with File Loading Option .....	60
Figure 46: Example template for window detection. ....	66
Figure 53: Voltage measured across LED array when pulsed.....	82
Figure 54: Measuring cone of light from LED array .....	83
Figure 55: Cropped region used for LED tests .....	83
Figure 56: Colormap of intensity values for LED array .....	85
Figure 57: Contours of colormap for LED array .....	86
Figure 58: Experiment Setup .....	87



## INTRODUCTION

One technique to better utilize existing roadway infrastructure is through the use of HOV and HOT lanes. A system to monitor the use of these lanes would assist in the operation and management of these assets. The ability to access usage would be beneficial to management and planning. The main goal of this research effort was to access the possibility of determining passenger use with imaging technology. This is especially challenging because of the changes in the type of glass being used by the car manufacturers to reduce the solar heat load on the vehicles. The aim of the glass modifications is to reduce overall energy transmitted through the glass outside of the visible wavebands and thereby reduce the energy usage in the vehicles especially for cooling. This would also have the additional effect of reducing the generation of greenhouse gasses.

This goal is also reflected in the transmittance standards for the proposed California Cool Cars regulations which are summarized below. The aim is to reduce the production of greenhouse gasses by reducing the loads on automobile air conditioning systems. This in turn will affect the suitable wavelengths for sensing people in vehicles. The guidelines will require that Tts (The total solar transmittance) allowances for new vehicles achieve the following levels.

- By 2012 75% of windshields must have a  $Tts \leq 50\%$
- By 2013 100% of windshields must have a  $Tts \leq 50\%$
- By 2014 100% of windshields must have a  $Tts \leq 40\%$

Tts is defined as: ratio of the transmitted solar flux to the incident solar flux

Earlier attempts at using imaging utilized energy in the IR (infrared) wavelength bands. With the proposed changes in the types of glass these systems will now be hampered in their ability to provide the desired functionality.

The main goal of this effort is to assess the possibility for sensing in vehicles that are using the current types of glass as well as the possibility for automated processing and counting under these conditions.

Detecting and automatically counting vehicle occupants using a visual camera pose numerous challenges such as reflection from the windshield, different operation conditions, and shadows. Most of the work in this regard uses a combination of visual and near infra-red (NIR) range. NIR is almost completely transmitted by the vehicle windshields. Following is a brief description of the state of the art in automatic detection of vehicle occupants.

### **Background**

The work proposed would build on the knowledge and experience obtained from a previous GDOT research project conducted during 1995-1998 titled "Computer Assisted Infrared Imaging System for Determining Vehicle Occupancy" (called GVOS for Georgia Vehicle Occupancy System). The goals of that study were twofold: the primary goal was to develop and demonstrate new technology for planning data collection, and a secondary goal was to determine the feasibility of the approach for HOV enforcement. GTRI developed and demonstrated a system that accomplished the desired goals. A

sample image acquired at highway speed on I-285 using this first-generation system is shown in Figure 1.

As part of the study, we also conducted a test using observers on the roadside compared to observers using images acquired by the GVOS system. A total of 200 images were recorded in the car-by-car tests. The vehicles in this sample were carefully selected by the observers, who believed that they had a clear view and that they could accurately determine occupancy and seating configurations in each case. Their observations were recorded on paper forms. The corresponding GVOS image data was later examined in the laboratory and scored in the same manner, by two persons using the same paper forms as the roadside observers.

Of the 200 GVOS images, 179 (90 percent) were useful and 21 were not, due to misfires. When the 179 images were scored in the laboratory, one observer's data agreed with the roadside data in 95 percent of the cases, while the other observer agreed in 93 percent of the cases. The comparison also revealed another interesting fact: in four cases (2 percent), the GVOS images clearly showed children in the back seat who were not recorded by the roadside observers. We concluded that the GVOS system provided the capability to accurately determine vehicle occupancy.



Figure 1: Passenger in Vehicle.



Figure 2: Extracted Passenger in Vehicle.

The system utilized invisible, near infrared (NIR) light (greater than 850nm wavelength) that was provided by a Xenon strobe with a short flash duration (1/10,000 second). The camera used was a low-light-level, intensified camera. It collected data of all of the vehicles in the lane being monitored. For each vehicle, the system produced an infrared (IR) flash and recorded an image with the IR camera that was digitized with a PC frame grabber. This data was then stored for later retrieval and visual analysis. This system demonstrated that it was possible to acquire images at 80 mph that would be suitable for HOV occupancy determinations with human analysis. As part of this proposed effort, we would develop a tool to automate this analysis process to reduce the workload on the operators.



In addition, the technical opportunities and challenges have changed somewhat during the past eight years, thus driving the need for a modified solution. The most significant change is an industry trend toward a new type of automobile glass that has been modified to reduce the transmission of IR sunlight as a means of reducing the heat load on cars during the summer season. This means that the earlier system using an IR flash in the 859 nm wavelength has limited practicality as that system would not see into many vehicles that had glass with reduced IR transmission. A sample plot of the transmission spectrum for this new glass is presented in Figure 3. It can be observed that in the near IR (900 – 1400 nm) the transmission of ambient sunlight and the earlier system's IR flash strobe are significantly reduced, thereby hindering the ability to sense energy in these wavebands in order to acquire an image.

It is proposed under this study to develop and evaluate a system that would function close to the 700 nm limit of the visible spectrum. This will require the design of a system that includes the sensing and illumination elements needed to acquire images at the proposed new wavelengths.

## Solextra<sup>®</sup> Vision Glass

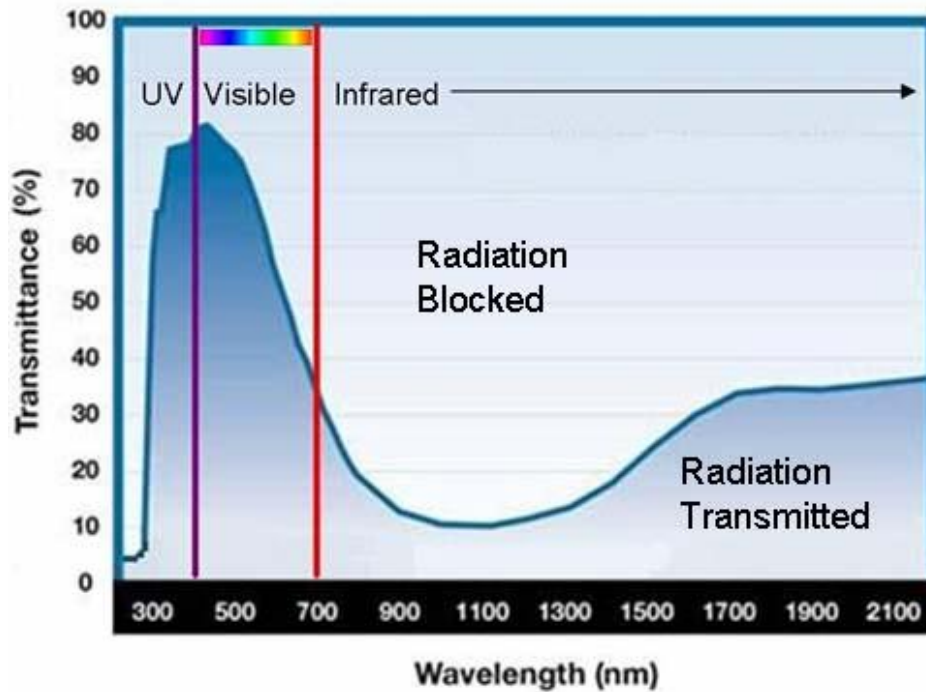


Figure 3: Transmission Properties of Infrared-blocking Automobile Glass.

A review of the technology in a study conducted by the Texas Transportation Institute (TTI)[7] indicated that at the time of writing there was one commercial system under development utilizing a dual band sensing approach: one in the visible and one in the NIR. The system known as Cyclops is manufactured by Vehicle Occupancy Ltd. in England. The study, however, indicated that the device needed improvements to be considered sufficiently accurate and reliable based on field trials. The company's current website describes the system, but technical details on its operation and performance are not known at this time.

The study also investigated certain within-vehicle occupancy technologies whose primary purposes were for other reasons such as the intelligent control of seatbelts. These technologies might potentially be used with a second purpose being occupancy data acquisition. It has been proposed that some of these other technologies might be utilized, but there is no current infrastructure to make this data available for monitoring vehicle occupancy[5]. Developments underway might make this possible in the future, but they will take years to bring into practice, require significant infrastructure upgrades, and it would probably not be feasible to retrofit older vehicles. A system such as the one being proposed that is capable of roadside monitoring of vehicle occupancy is vital for providing the data needed for the proper management of HOV operations. As part of the TTI study[7], researchers also investigated the range of technologies that could be used for Roadside Monitoring and identified the use of near IR as one of the more promising technologies based on somewhat generic operational specifications. The results of the comparison from the TTI study are presented in Table 1. By this analysis, a near IR system solution is the only one that meets the stated specifications. This conclusion supports our proposal to build on the earlier Georgia Tech work and develop a system to function in the near IR spectral region in the vicinity of the 700 nm wavelength. The study will evaluate the requirement that the system will operate under the desired environmental conditions while not being a distraction to drivers.

Table 1: Performance Comparison of Roadside Occupancy Detection Technologies.

<b>Desirable Property</b>	<b>Visible Light (Passive)</b>	<b>Near Infrared</b>	<b>Thermal Infrared</b>	<b>UWB Radar</b>	<b>Microwave</b>
Not blocked by tinted vehicle windows	N	Y	N	N	N
Capable of all-weather and night-time operation	N	Y	Y	Y	Y
Capable of resolving vehicle cabin details	Y	Y	N	N	N
Fast enough to capture vehicles moving at freeway speeds	Y	Y	Y	N	N

Other technological advances beneficial to the study effort include: reduced cost cameras, more controllable illumination sources, as well as the reduced cost and improved capability of current computer systems. These developments should allow for a more cost-effective implementation than the prototype developed in the previous research effort. The other element of this project will be to begin development of an image processing program to support people counting for evaluation of the system. Preliminary work indicates that tools could be developed to support the automatic counting of people in the vehicles as illustrated in Figure 1 and Figure 2. Figure 2 was obtained by processing the digital image in Figure 1 to highlight the driver. Further processing would be utilized to perform counting, for example, by looking at the shapes and other features in the window area. It is anticipated that most of this development would be conducted in the Phase 1 part 2 activities described below.

A review of current options found no system able to fully accommodate the proposed changes. Detect provides a commercially available automated system for determining the number of occupants within moving road vehicles (<http://www.vehicleoccupancy.com>.) The system projects two low intensity beams of Infrared (IR) light of different wavelengths onto the vehicle. Two digital photos are taken and merged to produce a single image and then processed by software based algorithms to detect the number of people.

Similarly in (Hao, Chen, Yao, Yang, Bi, & Wang, 2010), the authors use the near infra-red (NIR) illuminator to illuminate the interior of the car and a digital photo is captured using a camera equipped with an NIR filter. This setup reduces the effect of reflection of light from the windshield of the car. The captured photo can be viewed by a human screener or processed by computer vision algorithms to determine the number of occupants. Other work that uses the NIR range is (Wood, Gimmestad, & Roberts, 2003). Alternate to NIR range is to use thermal imaging systems to detect occupants using their heat map. However the use of athermal metallic coatings on the glass prevents the penetration of these wavelengths through the windshield. The changes being proposed in the windshield specifications would pose operational problems for the aforementioned systems. The main goal of this work is to develop and evaluate a technique to allow systems to operate under these conditions and to provide the data and information needed to support the operations on HOV/HOT systems.

## PROCEDURE

This study will look at the two main elements of the system. These are: Sensing and Processing. In addition there is testing of the proposed approaches and the generation of a conceptual design of a test system that could be installed for evaluation under operational conditions. The report will be structured as described below in the section of titled Findings.

### Sensing Aspects:

- Geometry
- Trigger selection
- Imaging
  - Window studies
  - Camera selection
  - Optics/Illumination

### Processing Aspects:

- Overall control system software
- Image Processing Software

### System Testing

- Street Data acquisition
- Highway data acquisition

### Processing/Analysis

### Conceptual Design System for Field Testing

- Hardware
- Software

## **FINDINGS**

As presented earlier the work will be conducted in the areas of Sensing, Processing, Testing and the Generation of a conceptual design. The sections that follow will address each of these aspects.

### **SENSING**

The work on the sensing area looked at the geometry involved in the system design. In addition the imaging optics, of identification and selection of a trigger, camera and processing unit are covered.

#### **Geometry**

It is required of this system that we be able to access the number of occupants in the vehicles. We therefore had to have view angles that allowed us to see passengers as currently the assumption could be made that there is a driver in the vehicle. In order to meet the needs of HOT types of operation it is necessary to be able to look in the back seats of vehicles as one HOT requirement will be that there has to be at least three people in the vehicle. Using a utility called Google Sketch Up we were able to generate CAD representations of the potentially different site configurations, poses and orientations of the cameras as shown in Figure 4. This also enabled us to estimate working distances and field of views that provided the parameters needed for our optics calculations.

We initially considered a heads on view but changed to a more frontal/side view that provided a view of the rear seat of the vehicle. An example is shown in Figure 5.

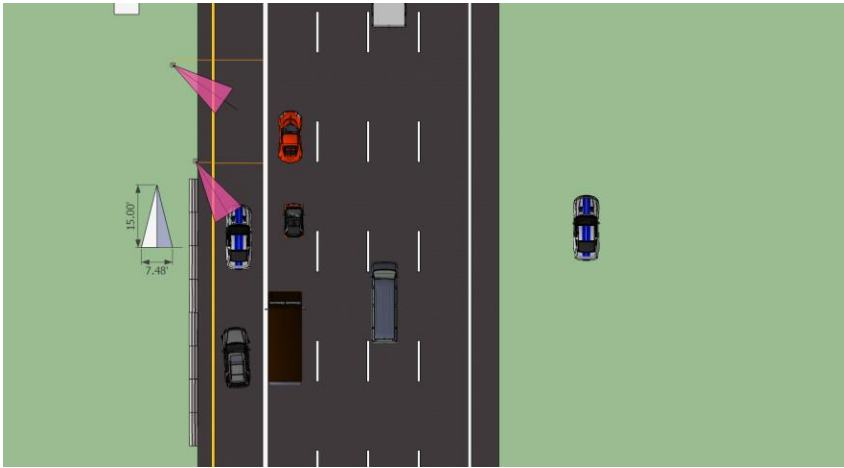


**Figure 4 Overhead view of Potential site using Google Sketch Up**

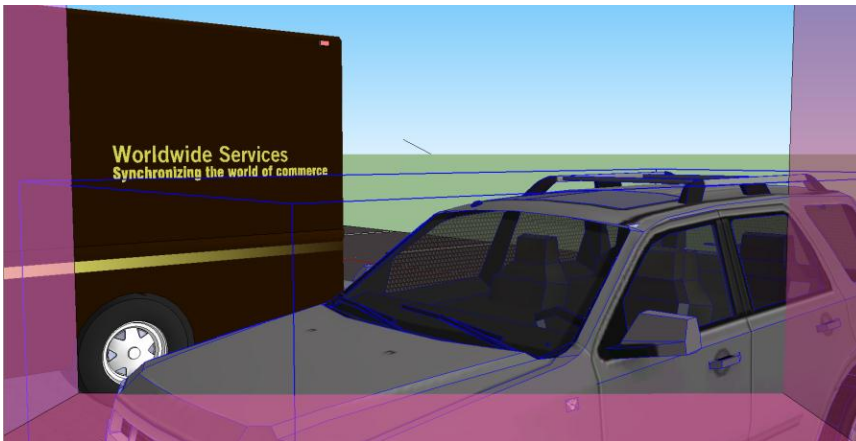


**Figure 5 Example view angle providing view of rear seat**

We visited a potential test site for a demonstration system at I-85 and Pleasant Hill road as suggested by Mr. James Gordon with the GDOT.





**Figure 6 Potential test site for demo system**

Using data from the site visit and the Google Sketch-up we completed the specification of the camera lens. In addition we discussed a technique for triggering the system and settled on an IR range finder for the system trigger.

We also had an interest in the angles of incidences that would occur based on the possible geometries and conducted tests to determine their effects.

### **Trigger Selection**

We selected an MDL Laser Systems ILM OEM laser module for this project. It is capable of measuring range, speed and height of vehicles. The device operates under the principle of time-of-flight. There are two windows on the front end of the laser. One

window emits a short pulse of eye safe radiation and the second window, which contains a photo detector circuit, collects the reflected light. The distance is calculated by measuring the time it takes the light to reach back the laser module. The laser was selected because it can work to a 1 square meter target at a distance of 150m at 200 Hz. It was also eye safe. The selected laser is already being used in security, construction and aviation markets. However, in practice there are several factors that define how well the laser will work, such as the target reflectivity, size of the target and distance of the target.

One issue that needs to be addressed is that the laser did not trigger in a timely manner in about 10% of the vehicles. In some cases it triggered late and in some it did not trigger at all. Mostly these were dark and shiny color vehicles. During the experiments it was noted that if the distance between the laser and the vehicle is more than 15m, the laser captured 100% of the vehicles. At closer distances, about 10% of the vehicles are missed. We think it is due to the use of round (pencil) laser beam. At shorter distances the laser beam is too focused and sometimes may hit the vehicle at an angle where all light is scattered and nothings reflects back. This problem can be alleviated by using a fanned laser module, which forces the beam to diverge in the vertical plane. In the horizontal plane, the laser beam remains collimated. Figure 8 shows a picture of fanned laser module.

## **Imaging**

### *Window/Glass Studies*

One of the motivating factors for this work is the knowledge that car makers were moving to types of windshield and window glasses with the capability for rejecting more of the solar load. One of the first tasks was to test samples of current windshields to observe their transmittance. A test apparatus was designed as shown in Figure 7. The output from this apparatus was compared to the output from a standard lab spectrophotometer for several samples and shown to produce representative results. This data is presented in Figure 8 for a CARY spectrophotometer and our device. Using our apparatus several wind shield samples were tested to obtain the transmission plots as shown in Figure 9. We are able to see the fall off in transmission above 780 or so nanometers in most of the models. This supported the need for an illumination system that could penetrate the vehicle while still being unobtrusive. A system using IR as in earlier demonstrations would not function under these conditions. A system to penetrate the vehicle while being somewhat unobtrusive to the drivers was needed for this problem. Our strategy is to design a system that would allow us to operate just outside of the visible region in a 'strobed' mode to reduce the potential to distract the drivers.

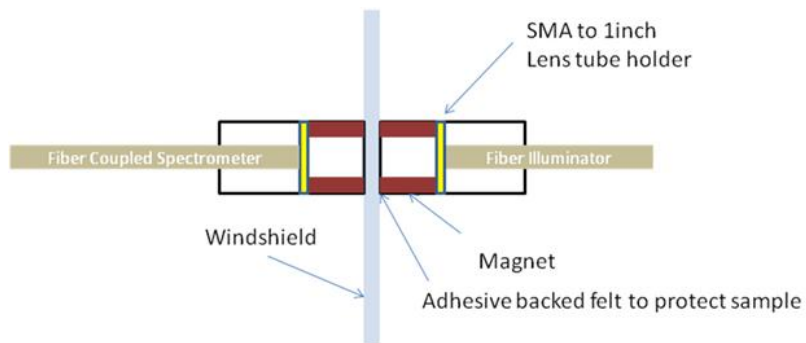


Figure 7 Design for Glass Transmission Measurement System

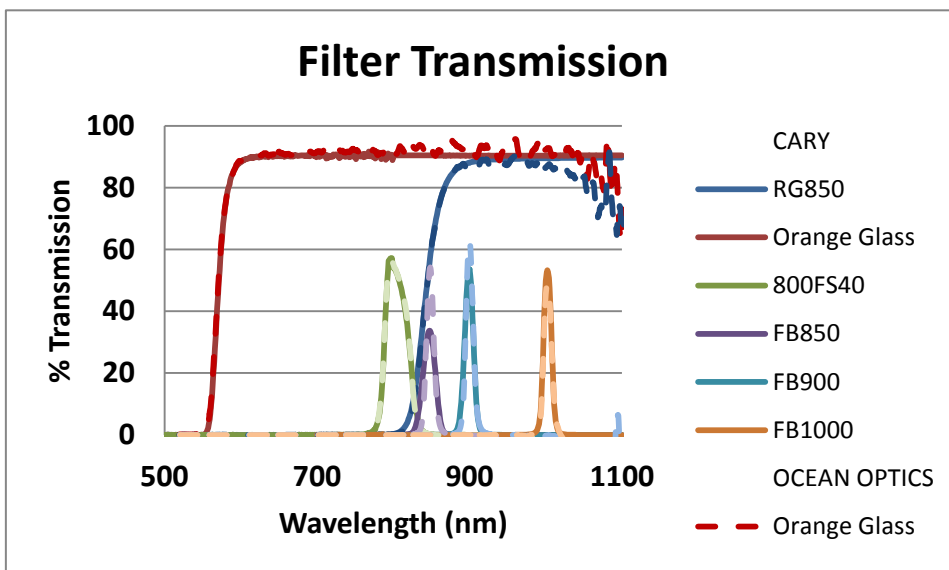
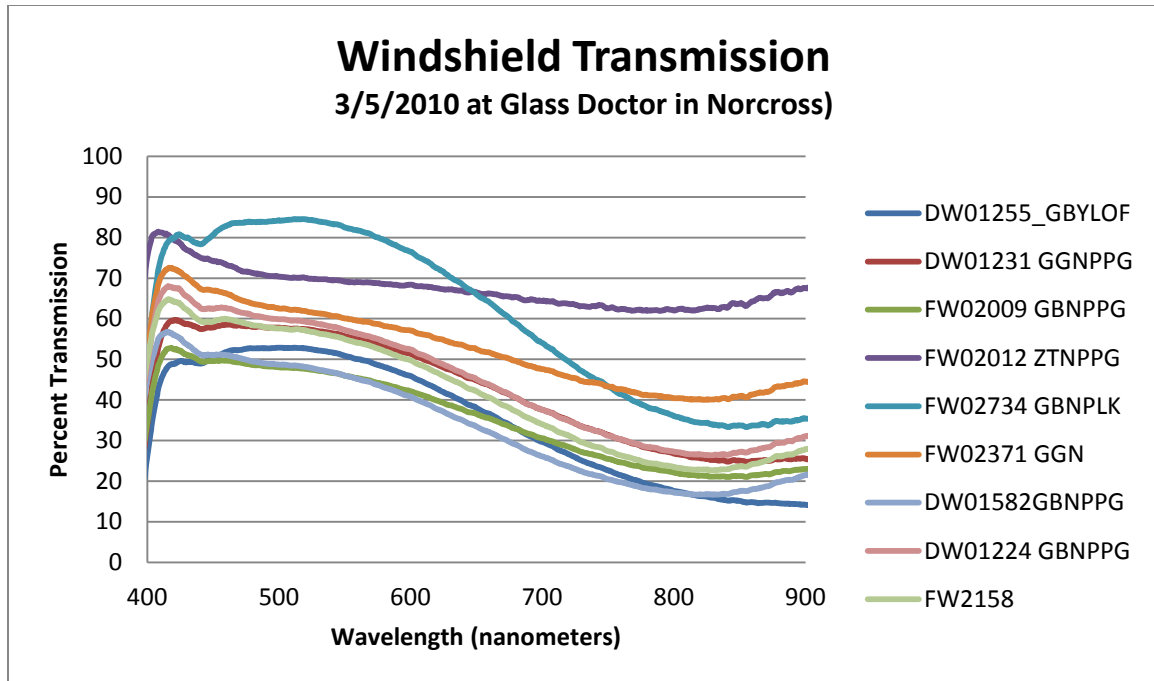


Figure 8 Comparison of transmission measurement apparatus with CARY spectrophotometer



**Figure 9** Transmission data from samples of commercially available windshields

We also began looking for sources of illumination that could provide energy in the wavelength bands required to penetrate the vehicles.

### *Camera Selection*

Based on the requirements for the sensing we chose a Point Grey monochrome Chameleon camera with a response up to 850 nm. The general idea is that the cutoff for the windshields would never be perfect so that there is always likely to be some transmission in the wavelengths a little above the visible portion of the wavelength bands. The ability to acquire data at these wavelengths would make the system unobtrusive to the drivers. The Point Grey Research Chameleon CMLN-13S2M adheres to the IIDC 1394-based Digital Camera Specification v1.31 but features the USB 2.0

interface. The black and white 3.75 by 3.75 micrometer CCD (ICX445AL 1/3" EXview HAD) supports frame rates of up to 18 frames per second at the maximum resolution, 1296 by 964. It is exceptionally small at only 25.5 by 41 by 44 mm, weighs a mere 37 grams and can be mounted with a standard 1/4"-20 bolt. It uses the standard CS-mount for optics. It also features 7 GPIO (General Purpose Input/Output) pins: 4 for external triggering and strobing, a +3.3v to power external circuits, an external power source and a ground pin. Our camera's Serial Number is 10060265, has an IIDC Version of 1.31 and a Firmware Version of 1.2.2.3. The spectral response for the camera sensor is shown in Figure 10. A camera with a better response at the wavelengths of interest would improve our signal.

### Monochrome Model

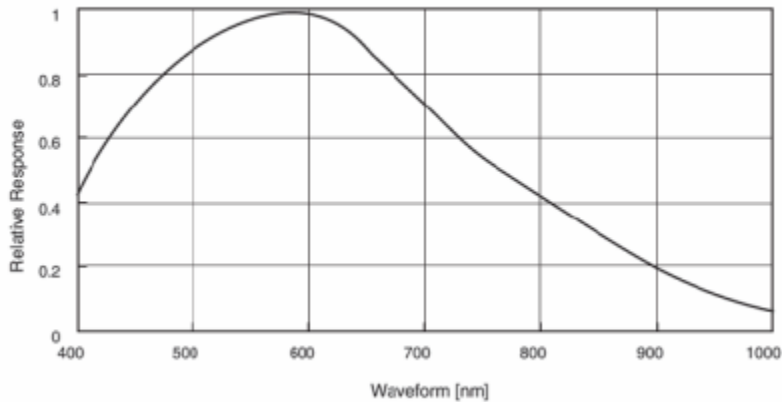


**Figure 10 Spectral response of the monochrome Chameleon camera**

## *Optics and Illumination*

Our initial tests using LEDs for illumination indicated no commercially available source that would be adequate for our needs. As a result we decided for our tests to use a Xenon IR illuminator that is capable of producing enough energy in the wavelengths of interest for testing. Will continue to pursue possibilities for an LED solution (this would be more reliable, cost effective and provide a more desirable form factor for a deployable solution). We purchased a VIGI-Lux MVS5770 IR Illuminator from Perkin Elmer. After delivery we performed tests on the illuminator to determine suitability for the application. The results are shown in Figure 11 and Figure 12. The green line in Figure 11 shows the response of the filter to be used on the camera to reduce the influence ambient solar insolation. The results indicate that the power output should be adequate for our tests. We did notice a visible flash when we fired the strobe. This does not match the expected performance as it would be a distraction to drivers especially at night. It turned out that the filter was cracked and returned to the manufacturer for repair. The illumination system performed according to the specifications after repair.

# Vigi-Lux MVS 5770 IR Illuminator Absolute Irradiance on a 600 Micron Diameter Fiber

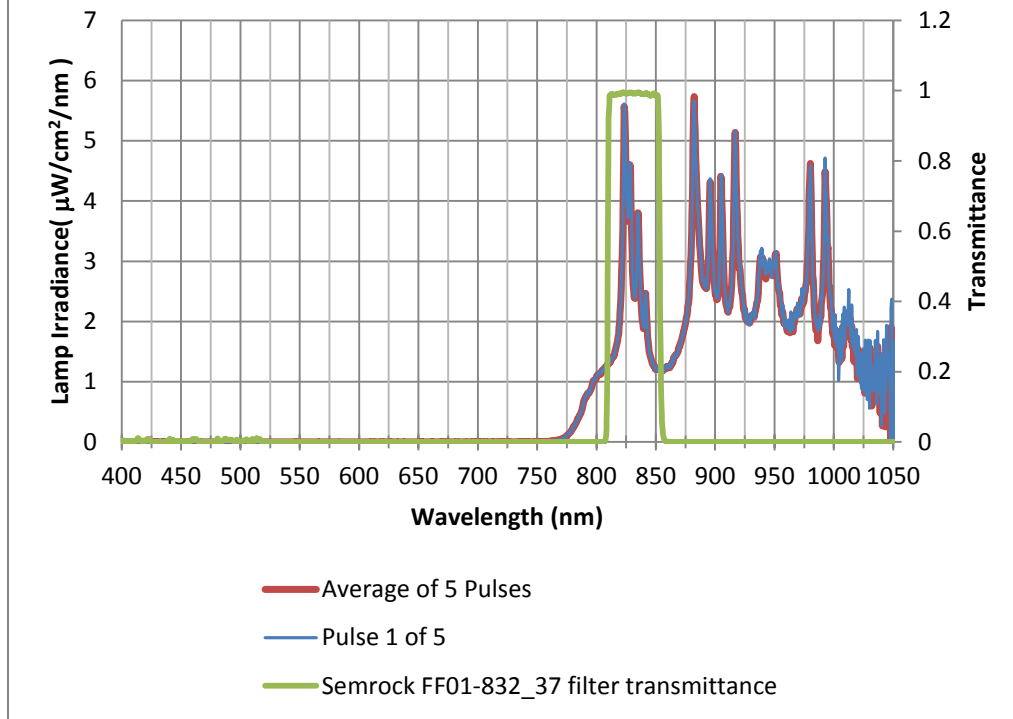
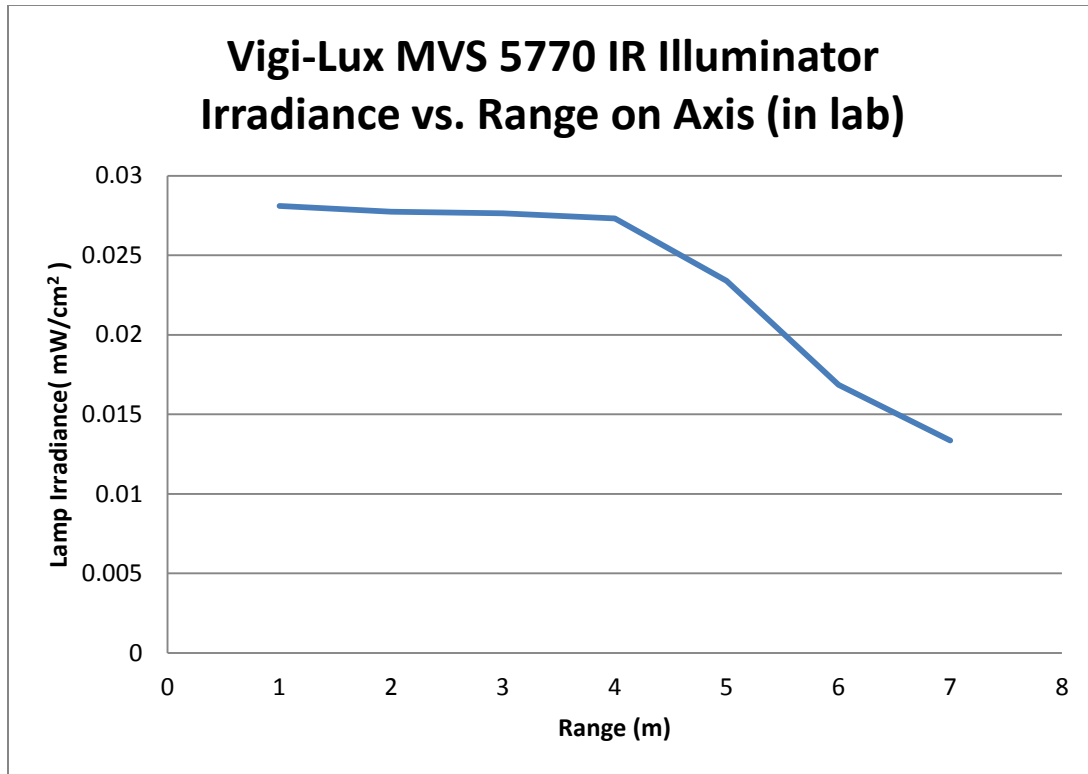


Figure 11 Perkin Elmer MVS 5770 IR Illuminator spectral output





**Figure 12 Perkin Elmer MVS 5770 IR Illuminator power output vs. range**

An analysis on the eye safety at the desired working distances and modes of operation was also tested. The analysis showed the system to be safe for the wavelengths to be employed and the desired strobe durations. Also in Figure 11 is the plot of the band pass (Semrock) filter used on the camera. This is necessary to freeze motion of the vehicles and also reduce the effect of solar radiation at daytime as with longer integration times the solar radiation would overcome the source and impede our ability to see inside the vehicles.

There was some concern about using the Xenon source in the long term both from the viewpoint of the life of the device as well as the potential safety of the source. The main safety concern is that since it is a filtered Xenon source if the filter is broken it could potentially temporarily blind motorists. As mentioned earlier we looked at LEDs as potential sources which would require us to drive them at fairly high currents to get the power needed. The potential benefits would include a longer life as well as more accurate control of both the illumination spectra as well as the on/off cycles. This solution would also provide some flexibility in the form factors that could be used for the illuminator to make it less observable. We therefore did some testing using a bank of commercially available devices to estimate the numbers that would be needed to at least match the Xenon strobe. We estimate that it would take ten of this bank of LEDs running at high current to match the output from the Xenon strobe. Please see the relevant section in the Appendix for more detail on the testing.

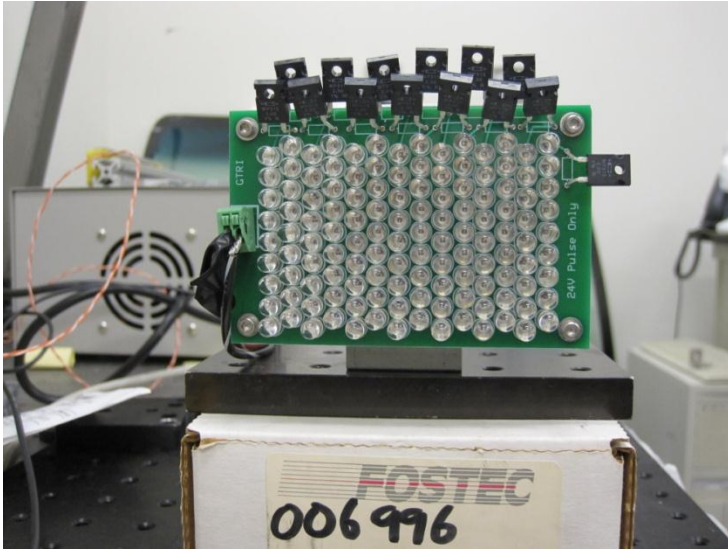


**Figure 13** Sample Illumination LED array

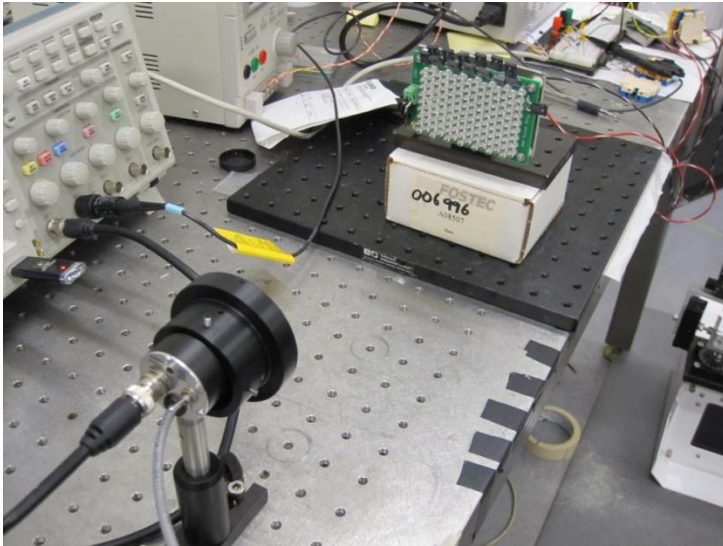


**Figure 14** Test apparatus for LEDs

### *Incident Angles*

We also anticipated that we would have to image through the windows of the vehicles at a variety of incidence angles based on the types of vehicles as well as the position at

which the image acquisition was triggered. We therefore did a study to access the potential effects. This was accomplished by using the apparatus shown in Figure 15 to image a black and white target to determine or ability to see the target at different orientations.



**Figure 15 Transmission measurements at various orientations**

The results shown in Figure 16 and Figure 17 indicated that windshield angles up to about 30 degrees in yaw or 45 degrees in pitch we don't see appreciable changes in the pixel values for the white and black pixels of the target. This means that for the geometries under consideration the sensing should not be adversely affected by windshield configuration.

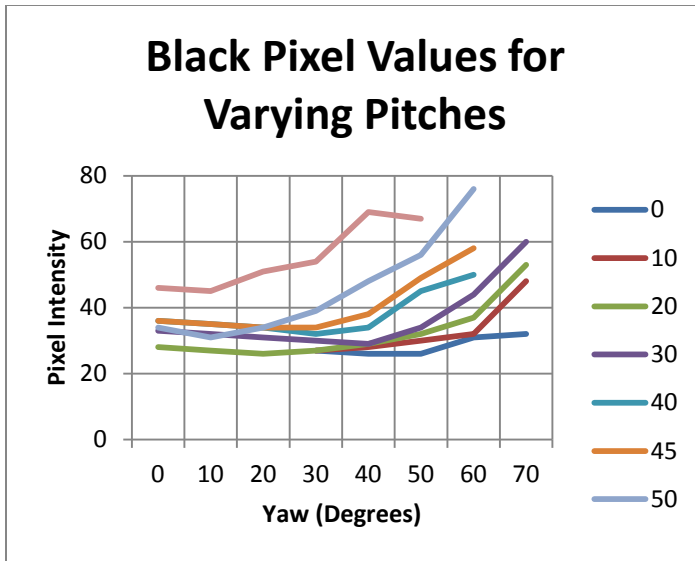


Figure 16 Effect of pitch on transmission

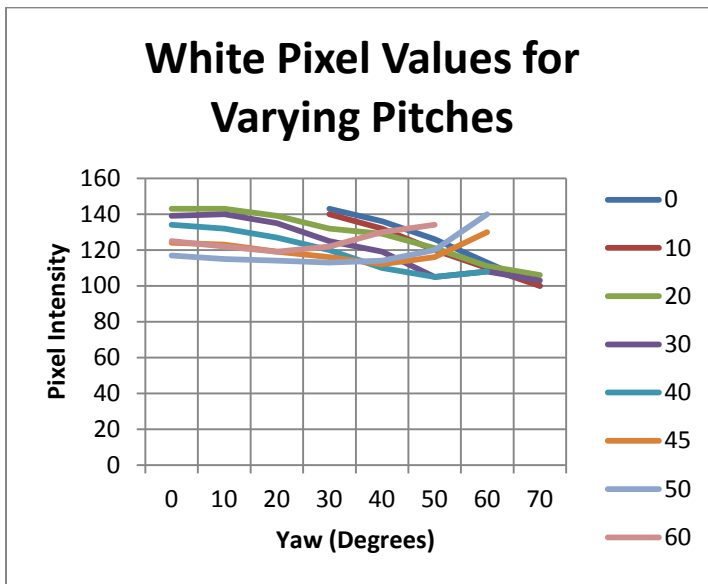


Figure 17 Effect of yaw on transmission

## PROCESSING ASPECTS

The system as designed and tested is shown in Figure 18. It consists of the illuminator, the camera sensor and a vehicle trigger to start the acquisition operation whenever a vehicle is in the specified range of the system. The test area behind one of the GTRI buildings is shown in Figure 19 and the sample vehicle used for the initial tests in Figure 20. Sample output images using this initial system are shown in Figure 21 and Figure 22. It is apparent that at least for these vehicles it is possible visually to detect the occupants of the vehicle. Some of the initial tests looked at using a view that was more head on. We modified this geometric representation for two reasons: one to be able to get a better view of the rear seat of the vehicles and also because the front view gave less repeatable images probably because of the wider range of geometries so that there were more specular reflection effects that hindered a view inside the vehicle.



**Figure 18 Initial System configuration IR illuminator t a laser trigger and camera.**



**Figure 19 System undergoing initial testing**



**Figure 20 GTRI Sample vehicle**



**Figure 21 Sample output image**



**Figure 22 second sample image**

## **CONTROL SYSTEM SOFTWARE**

In addition to the sensing work software was developed to support system testing data acquisition and analysis. The graphical user interface (GUI) developed for the software application is shown in Figure 23. The functionality derived from the software can be



discerned from the different GUI elements but allows for the acquisition and storage of data in addition to the ability to run preliminary detection. Functionality was built into the GUI in to allow for control of the camera and imaging parameters. The main form controls whether any algorithms are to be performed on the input images and if the output should be saved. The Camera tab is used for snapping a single image, saving a single image, configuring the camera, and snapping and saving multiple images automatically.

The software also operated in an offline mode as shown in Figure 23. This GUI in is obtained by pressing the File tab on the first menu and is used for opening images in a directory and scrolling through them, or just selecting and opening a single image. Both options also implement the algorithm functionality and ability to view or save the output image.

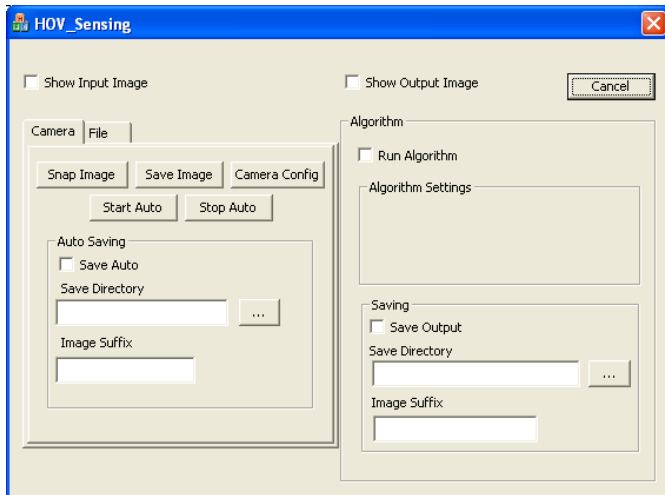


**Figure 23 Graphical User Interface to control the system**

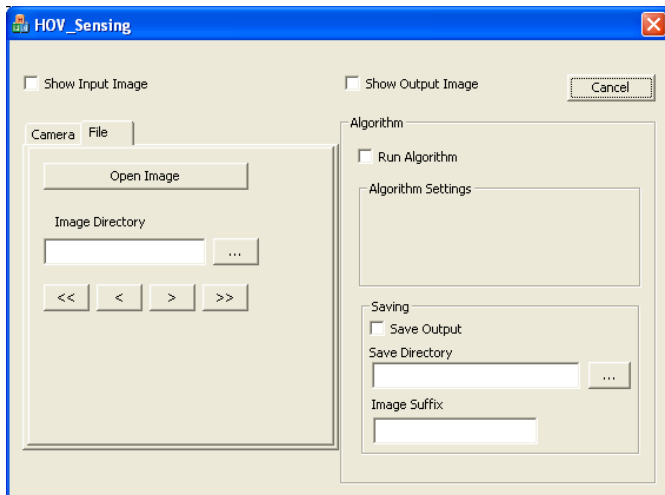


**Figure 24 Graphical User Interface for file viewing**

## **IMAGE PROCESSING SOFTWARE**

In conducting the evaluation one determining element would be the ability to automatically process the images acquired to detect the presence of people in the vehicles. This would be an integral part of the evaluation. Preliminary approaches to conduct this analysis were done as part of the overall assessment.

## SYSTEM TESTING

The next step was to obtain data for vehicles operating in their natural modes as would be seen on the roadway or interstate. We were assisted by researchers in the Department of Civil and Environmental Engineering at Georgia Tech to acquire data at sites representative of a surface street on the Georgia Tech campus and also on an interstate highway (Interstate 85 north of Atlanta). These two sites are shown in Figure 25 and Figure 26 respectively.



**Figure 25 Georgia Tech Test Site**



**Figure 26 Interstate-85 Test Site**

## Street Testing

The samples from the Georgia Tech campus are shown in Figure 27 and Figure 28. With the exception of a few missed triggers we seemed visually to be able to identify people in the majority of vehicles.



**Figure 27 Campus Sample 1**



**Figure 28 Campus Sample 2**

With the vehicles on I-85 we were able to see into most of the vehicles as shown in Figure 29 and Figure 30 but there were many vehicles such as shown in Figure 31 and Figure 32 that was difficult discern drivers and passengers.

**Interstate Testing**



**Figure 29 First I 85 Sample 1**



**Figure 30 First I 85 Sample 2**



**Figure 31 First I 85 Sample 3**



**Figure 32 First I 85 Sample 4**

This data showed the system to be capable of acquiring data in vehicles at Interstate highway speeds.

The system at the I-85 site is shown in Figure 26 and sample data is shown in Figure 29 to Figure 32 . It can be observed that it is possible to see the vehicle occupants example in Figure 29 and Figure 30. We noticed however that for some vehicles such as shown in Figure 31 and Figure 32 we were not able to penetrate the interior of the vehicles with enough energy to be able to discern the occupants of the vehicles.

We suspected that the issue was the working distance to the vehicles at the I-85 site which was on the order of 10 meters. We then did some further experiments to test this hypothesis.

### **Distance and Illumination Tests**

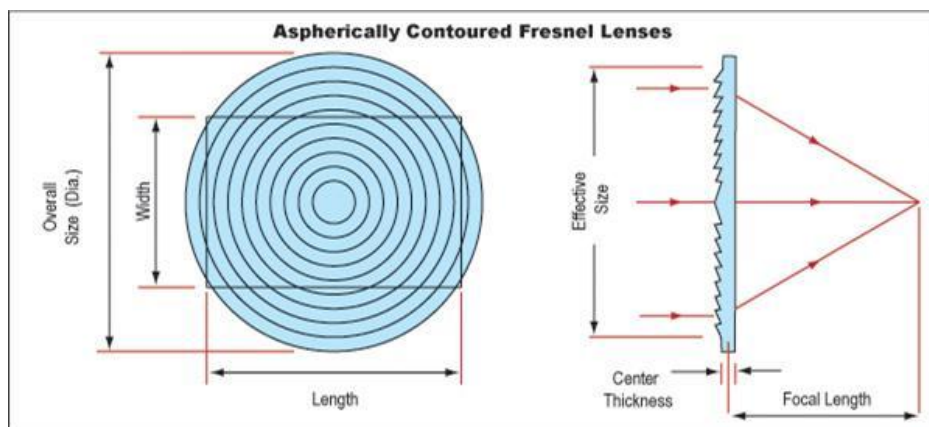
We suspected that the reason for the significant number of cars that we could not see in was due to the working distance and the lower power that was being delivered into the vehicle. We looked both the effect of the illumination pattern from the Xenon strobe as well as the working distance.

### ***Illumination Pattern Evaluation***

During early testing, one issue that surfaced was that we were not getting enough light onto target vehicles. We knew the output angle from the xenon strobe, and we determined that we were overfilling the targets, losing light around them. Since we are restricted as to how close we can get to the vehicles, we tested the idea of altering the output of the strobe.

We explored the possibility of adding optics to the xenon strobe in order to reduce the illumination solid angle leaving the output window of the strobe. This would concentrate light onto the vehicles. Less light would miss the vehicles and more light would pass into the vehicle interiors and reflect back to our camera. To keep weight, cost, and physical depth low, we tested a fresnel lens with the strobe. A fresnel lens is a thin version of a large diameter lens. It maintains its desired focal length but is dramatically thinner than a conventional lens. This is possible because the lens is divided into annular zones, and the thickness of each zone is reduced to the minimum needed to provide the desired optical power in that zone.

We tested a fresnel lens from Edmund Optics. It was 6.7" x 6.7" x .075" thick with a focal length of 3". Edmund Optics provides this image of a typical fresnel lens on their website (<http://www.edmundoptics.com/onlinecatalog/displayproduct.cfm?productID=2040&PageNum=1&StartRow=1>). The transmission of our fresnel lens was 92% in visible and near-infrared wavelengths.



To test the effect of the fresnel, we setup the strobe in a large, open room where we could control the ambient lighting. We aimed the strobe and camera at a wall nine feet away to mimic our field conditions. We recorded images as the strobe fired. We placed markers on the wall to indicate the edges of the illumination pattern. Control images were collected without the fresnel lens. Then the fresnel was added, once with the grooves pointed toward the strobe, once with them pointed away. The lens was approximately one focal length from the strobe's bulb. Our hypothesis was that the lens would nearly collimate the light leaving the strobe. What we found, however, was that the output dynamics of the strobe are complex. Not only does the strobe assembly contain a slender, cylindrical bulb, it also incorporates a large cylindrical reflector. The bulb and the reflector produced different effects through the fresnel lens, and the light pattern that resulted was less desirable than the pattern without the strobe. Examples shown in Figure 33, Figure 34, and Figure 35 are images captured of the wall nine feet from the camera and strobe. It can be seen that the image without the fresnel lens produced an illumination pattern that is rectangular and fairly homogeneous though larger than we desire. The patterns with the fresnel are shapes that are not ideal for our purposes, and they contain hot zones and shadows that would interfere with image processing. Our conclusion was that a fresnel lens is not the best method of concentrating light onto target vehicles.



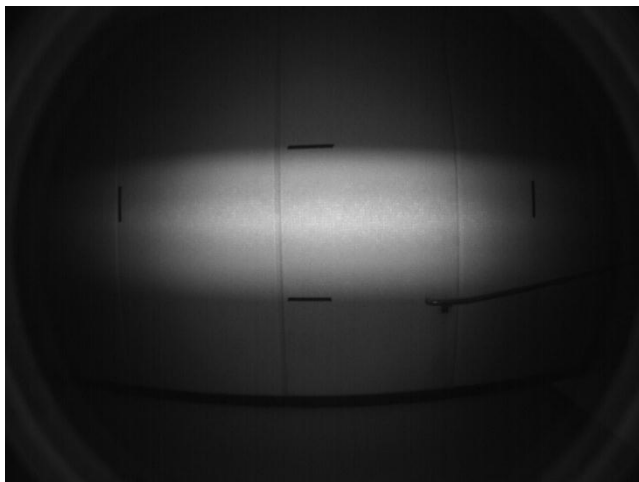


**Figure 33** Nine feet from wall, No fresnel

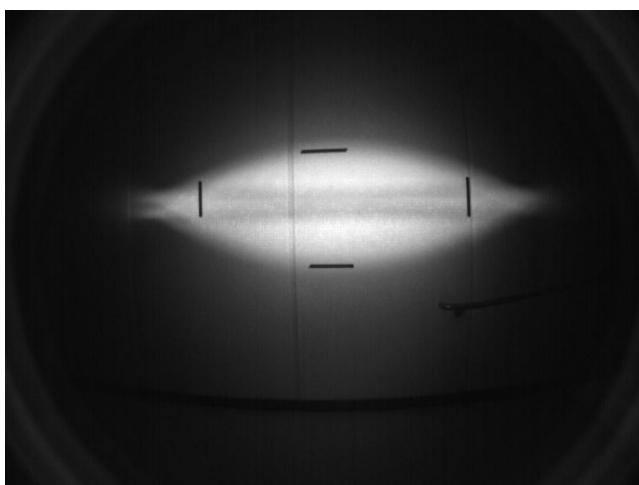


**Figure 34** – Nine feet from wall, Fresnel with grooves out (the prescribed usage orientation)

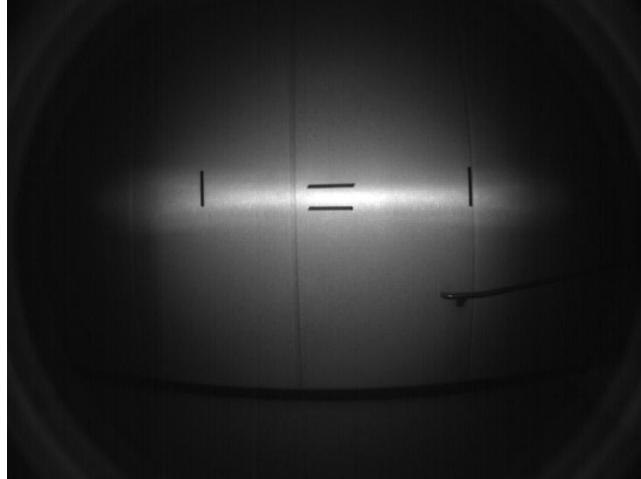


**Figure 35 – Nine feet from wall, Fresnel with grooves in**

### *Working Distance Tests*

For the working distance tests we positioned a vehicle at distances that corresponded to the ranges likely to be observed. The results of these tests are shown in Figure 36 and Figure 37 where we observe a significant decrease in the reflected energy from the inside of the vehicle as the working distance increased.



5 feet



10 feet



15 feet



20 feet



25 feet

**Figure 36 Reflected Energy at Different Distances**

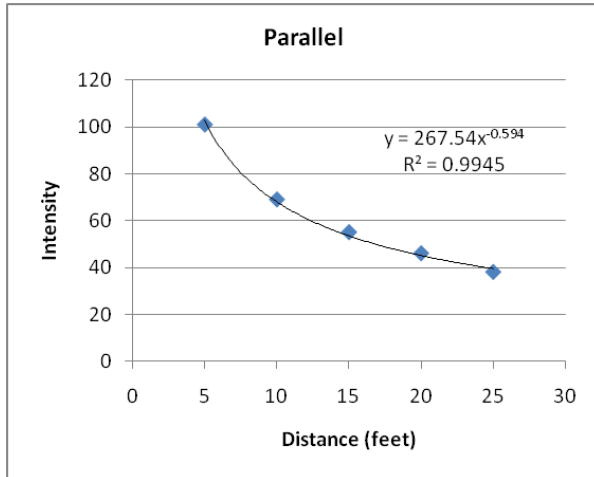


**Figure 37 Falloff in reflected energy intensity vs. distance**

As a result we decided to conduct another test at working distances closer to the ones likely to be used in a demonstration system with a working distance from the vehicles of 9 feet to 13 feet.

The results of these tests are shown in Figure 36 and Figure 37 where we observe a significant decrease in the reflected energy from the inside of the vehicle as the working distance increased. As a result we decided to conduct another test at working distances closer to the ones likely to be used in a demonstration system (9 feet to 13 feet).

## **I-85 Test Number 2**

We then made arrangements to return to the site to image on the exit ramp which would allow for a geometric configuration that was closer to the campus setup and more like what is likely to be experienced imaging from the median. Samples from this

location were acquired and we did not see vehicles that we could not discern the number of people in the vehicles as shown in the examples in Figure 38 and Figure 39



**Figure 38 Second I 85 Sample 1**



**Figure 39 Second I 85 Sample 2**

## **PROCESSING/ANALYSIS**

One of the goals of this system was to obtain data that could be automatically processed in order to be able to access HOV/HOT usage patterns. In the processing section we looked at the operations that would need to be done on the data to extract the needed elements.

Detecting vehicle occupants poses numerous challenges. We have taken a hierarchical approach to automatically detect people within the vehicles, where at the first level window regions are detected. In the second level only the window regions are searched to detect vehicle occupants.

Based on the results of the background research into the detection algorithms, we decided to look at four approaches for window regions and automated people detection. The approaches chosen for investigation are: Chamfer matching, SIFT (Scale Invariant Feature Transform) based detection, Haar and HOG features based detection. A more detailed explanation of the techniques and their use are presented in Appendix II.

In addition to the above mentioned methods, some other object detection algorithms were also tested. In light of the performance of different algorithms, we decided to use the HOG features for window detection and the Haar features for vehicle occupant's detection. Below we briefly summarize the advantages and disadvantages of the algorithms tested.

The Chamfer matching based algorithm required no training. However it required a lot of target object edge contours to give a reasonable detection performance. Having a large set of object edge contours affected adversely the speed of the detection algorithm. Moreover, catering for all the different shapes of the windows resulted in a set of edge contours that gave much higher false positive rate. One thing that can be done to improve the performance is to select the edges contours from among all possible contours using Adaboost as is carried out in (Jamie, Blake, & Cipolla, 2005).

Sample images and their processed outputs using the approaches described earlier are shown in. We demonstrated the ability to both locate the window regions of interest and to locate the presence of passengers in the vehicles. Sample output is shown in with more in Figure 40 where the region outlined in green identifies the window area of the vehicle and the region outlined in red people located in these regions. More work still needs to be done to automatically count people and also to assess vehicle adherence to HOV/HOT operational guidelines.



Figure 40 Sample processed output green region window red region people

### CONCEPT FOR DEMONSTRATION FIELD INSTALLATION

In order to fully prove out the concept for this system it would be beneficial to install a demonstration system at a site that would be somewhat representative of a typical



HOV/HOT installation. We would like to suggest the site at the I-85 Pleasant Hill Road exit ramp as a candidate. There are several reasons why this could potentially work well.

- There is an HOV lane
- There is a Hub Building with power and network access
- There are utilities located at the site

### **Hardware**

The idea would be to have camera and illumination system located remotely on the median at such a pose as to obtain the desired views into the vehicles. It might be possible to use multiple cameras to obtain more complete views inside the vehicles and to accommodate different vehicle types. These elements would then be connected to a control computer that would be located in the hub building where direct access to the GDOT and Georgia Tech Networks would be possible for system access as well as the management and storage of data. A graphic of the proposed installation is shown in Figure 41.

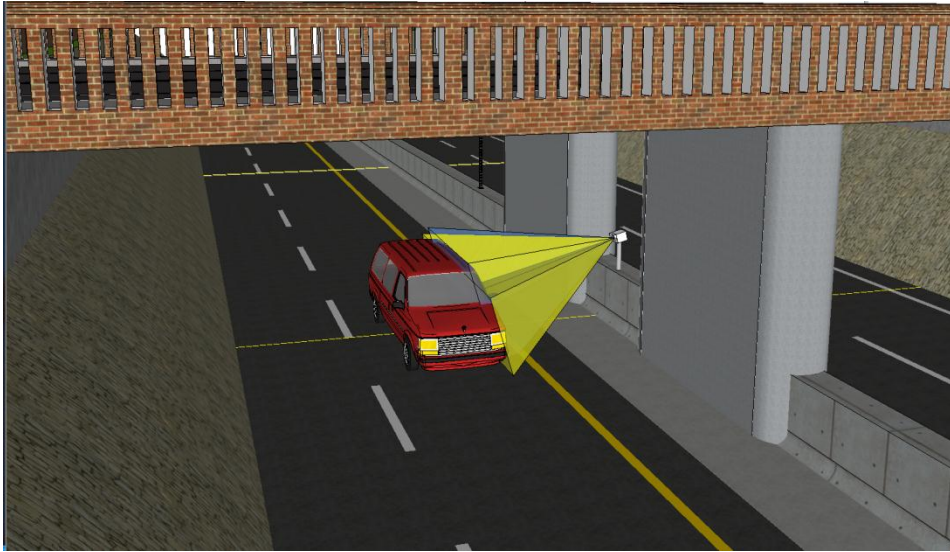


**Figure 41 Concept for demo system implementation**

### **Software**

We would plan to use the software developed under this first phase effort as the foundation for the overall system control and data analysis. This would allow us to control the remote devices and also to collect store and process the data to analyze various features or aspects of the data that would be useful for managing HOV/HOT lanes.

## **RECOMMENDATIONS**

This study has demonstrated the ability of the lab prototype system designed to sense occupants in vehicles on the interstate. The system can acquire data in vehicles that are travelling at highway speeds. The ability to automatically sense the passengers in the vehicle using image processing techniques was also shown. It appears that for

HOV/HOT solutions a view that is somewhat from the sides of the vehicle appears to give more reliable images in addition to allowing for improved observation of the rear seats which would be required for HOT applications as planned in Georgia. We have also looked at an alternate means of illumination using high powered LEDs. This appears to be a possibility and would provide aspect ratios for the system that might make it less obtrusive while reducing the possibility of distraction from the illumination pulse.

The approach described appears to be technically feasible and we recommend an evaluation at a representative HOV/HOT site such as the Pleasant Hill Road exit on I-85.

## REFERENCES

1. Goodin, G. *Enforcement of Managed Lanes with HOV Preference*. in *12th International HOV Systems Conference: Improving Mobility and Accessibility with Managed Lanes, Pricing, and BRT*, 2005. Houston, Texas.
2. Loudon, W.R. *Improving the Estimation of Potential Travel-Time Savings from HOV Lanes*. in *Transportation Research Board 86th Annual Meeting*. 2007. Washington, D.C.
3. Munnich, L.W. and K.R. Buckeye. *I-394 MnPASS High-Occupancy Toll Lanes: Planning and Operational Issues and Outcomes (Lessons Learned in Year One)*. in *Transportation Research Board 86th Annual Meeting*. 2007. Washington, D.C.
4. Poole, R., *A New Solution for HOV Occupancy Enforcement*, in *Surface Transportation Innovation*. 2007.
5. Schijns, S. and P. Matthews. *Automated Occupancy Monitoring Systems for HOV/HOT Monitoring and Enforcement*. in *12th International HOV Systems Conference Improving Mobility and Accessibility with Managed Lanes, Pricing, and BRT*. 2005. Houston, Texas.
6. Siegal, R. *Arizona May Open HOV Lanes to Lone Drivers*. 2007 [cited 2007 February 14, 2007]; Available from: <http://www.npr.org/templates/story/story.php?storyId=7407266>.
7. TTI, T.T.I., *Automated Vehicle Occupancy Technologies Study (Draft Synthesis Report)*. 2006. p. HOV Pooled-Fund Study Current Projects.
8. Turnbull, K.F. *HOV Lanes and Hybrid Vehicles*. in *Transportation Research Board 86th Annual Meeting*, 2007. Washington, D.C.

## BIBLIOGRAPHY

Dalal, N., & Triggs, B. (2005). Histograms of Oriented Gradients for Human Detection. *Computer Vision and Pattern Recognition*.

Fulkerson, B., Vedaldi, A., & Soatto, S. (2009). Class Segmentation and Object Localization with Superpixel Neighborhoods. *International Conference on Computer Vision*.

Gavrilla, D. (1998). Multi-feature hierarchical template matching using. *ICPR*, (pp. 439-444).

Hao, X., Chen, H., Yao, C., Yang, N., Bi, H., & Wang, C. (2010). A near-infrared imaging method for capturing the interior of a vehicle through windshield. *IEEE Southwest Symposium on Image Analysis and Interpretation*.

<http://www.vehicleoccupancy.com>.

Jamie, S., Blake, A., & Cipolla, R. (2005). Contour-Based Learning for Object Detection. *International conference on computer vision*.

Viola, P., & Jones, M. (2001). Rapid object detection using a boosted cascade of simple features. *Computer Vision and Pattern Recognition*.

Wood, J., Gimmestad, G., & Roberts, D. (2003). Covert camera for screening of vehicle interiors and hov enforcement. *SPIE-The international Society for optical Engineering*.

# APPENDICES

## Appendix I: Sample Output Images





# H.O.V. Sensing Software Design Document

---

**HOV Project Team**

**9/6/2010**



## Table of Contents

1. Goals
  - 1.1. Purpose
  - 1.2. Requirements
2. Class Overview
  - 2.1. Primary Classes
  - 2.2. Abstract Classes
3. Software Design
4. Abstract Classes
5. Algorithm Detail
  - 5.1. Occupancy Identifier
6. Software Operation
  - 6.1. Check Boxes
  - 6.2. Edit Boxes
  - 6.3. Buttons
    - 6.3.1. Snap Image
    - 6.3.2. Save Image
    - 6.3.3. Start Auto
    - 6.3.4. Stop Auto
    - 6.3.5. Camera Configuration
    - 6.3.6. Open Image
7. Database and Logging
  - System Configuration Items

## 1. Goals

### Purpose

The “H.O.V. Occupancy Sensing” project is primarily designed to detect HOV lane utilization. This is performed by using an imaging system to identify and calculate the number of occupants in vehicles in the HOV lanes in Atlanta, GA.

### Requirements

- Snap and save images of vehicles in motion at speeds up to 80 mph at rate of 1 per second
- Allow for review/processing of images saved
- Stub for processing images that can be modified as techniques are developed and enhanced
- Allow settings to be modified from xml file(s)
- Modify settings for trigger??
- Support for setup/configuration??

## 1. Class Overview

### Primary Classes

These provide the core functionality such as a graphical user interface, database functionality, and configurability through an XML configuration file.

- HOV\_Sensing – Creates the application instance and instantiates the dialog
- HOV\_SensingDlg – Creates, draws, and handles all dialog Interactions
- XMLConfiguration – Handles reading/writing configuration parameters
- QueueData – Handles logging of data to a database
- TabCtrl – initializes and controls dialogs within the tab control
- CameraDlg – first tab; handles camera operations (start, stop, snap, save, config)
- FileDlg – second tab; opens and scrolls through images from file

## Abstract Classes

These classes all inherit from one of two base classes, *GenericCamera* and *ProcessorInterface*. This allows for changing the acquisition method or processing engine with minimal software development overhead.

- Generic Camera – Generic camera interface that allows easy switching of hardware without changing any software calls (will have to change included interfaces).
  - *GenericCamera* – the generic class that includes very basic functionality that all cameras share.
  - *GenericImageFormat* –
  - *GenericCameraException* – Exception class used for error handling
- *PGRCamera* – Internally (FPTD) written PointGrey Research Cameras class that inherits from *GenericCamera*. It also contains a great deal of additional functionality specific to PointGrey cameras. Uses PointGrey's *FlyCapture2.0* library to communicate with the camera.
  - *CameraInternal* – Class hidden to the user. It includes and uses the *FlyCapture2* library. By using this “hidden” class, the end user only needs to include *CameraExternal* and the *PGRCamera* library in their project and do not have to include or link to any of the PointGrey source code.
  - *CameraExternal* – What the end user includes in the project and uses to access the camera. It merely “forwards” its calls to *CameraInternal*.
  - *CameraDefinitions* – A file to declare definitions that are used in the camera classes.
- *ProcessorInterface*
  - *OccupancyIdentifier*

## 2. Software Design

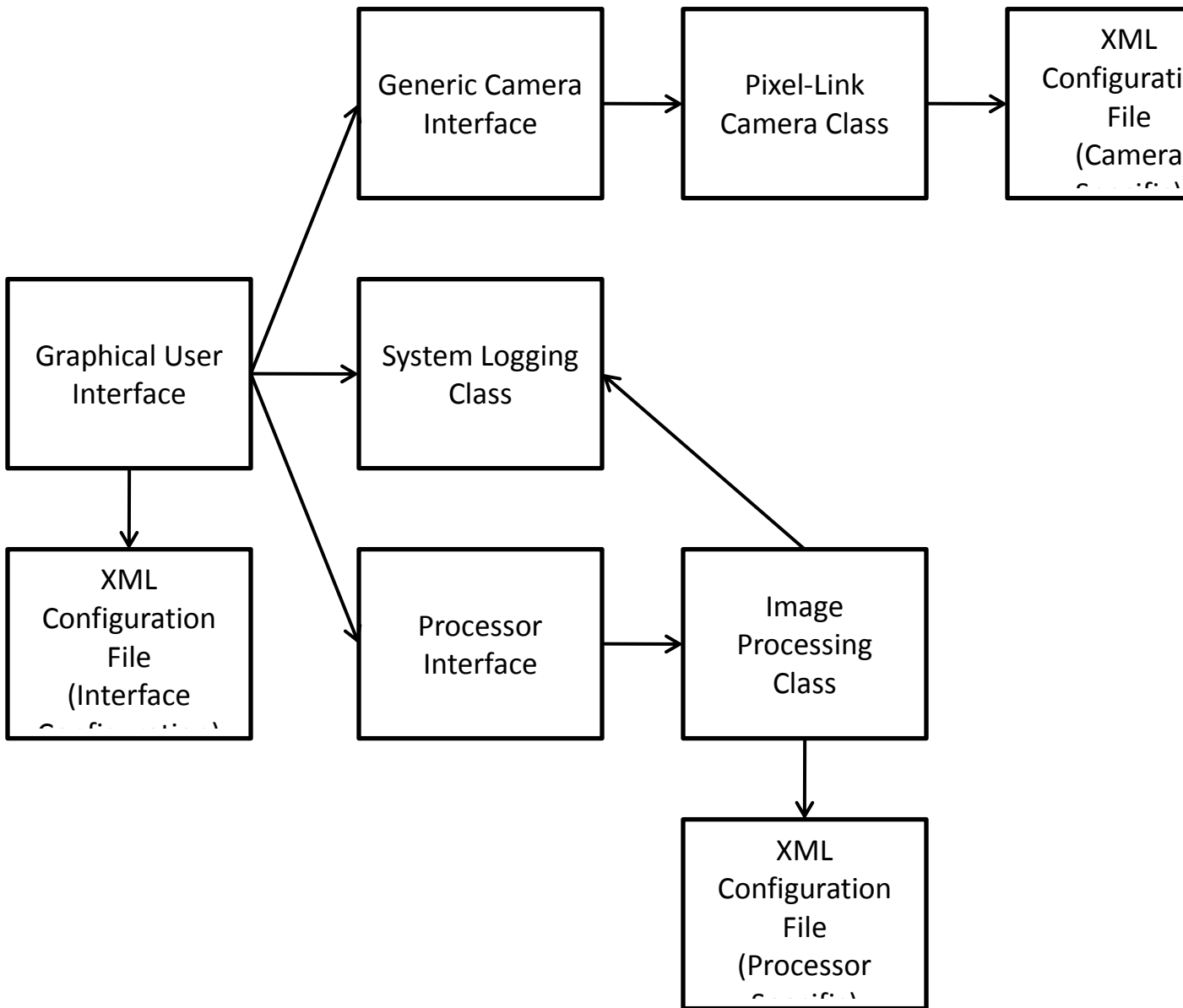


Figure 42 - Software Design Block Diagram

### Camera Initialization

There are several steps to setting up the camera. The reasons behind them are detailed in Appendix II. There are two categories of parameters to initialize, Camera Settings and hardware parameters.

The current camera settings initialized are:

Setting	Value
Shutter	.16 ms
Gain	22 dB

All others (Brightness, Exposure, Gamma, etc) are turned off.

The hardware initialization is done next. It sets the camera into the correct trigger mode, sets up the external trigger and strobe, and sets the delays and durations to their ideal values.

Additionally, the snap call actually turns the strobe on and off to prevent the light source from triggering when the system is not taking a picture.

## **Software Operation**

The program is a Dialog Based MFC program; therefore, all functionality is driven by user interaction (button clicks, check boxes, etc.) A single function named *DoProcess*

will perform the actual image processing tasks required by the system. Figure 2 shows a flowchart of the *DoProcess* Functionality. Figures 3 and 4 illustrate the dialog. The following sub-sections will detail the functionality of each button, edit box, and check box, using flowcharts where appropriate.

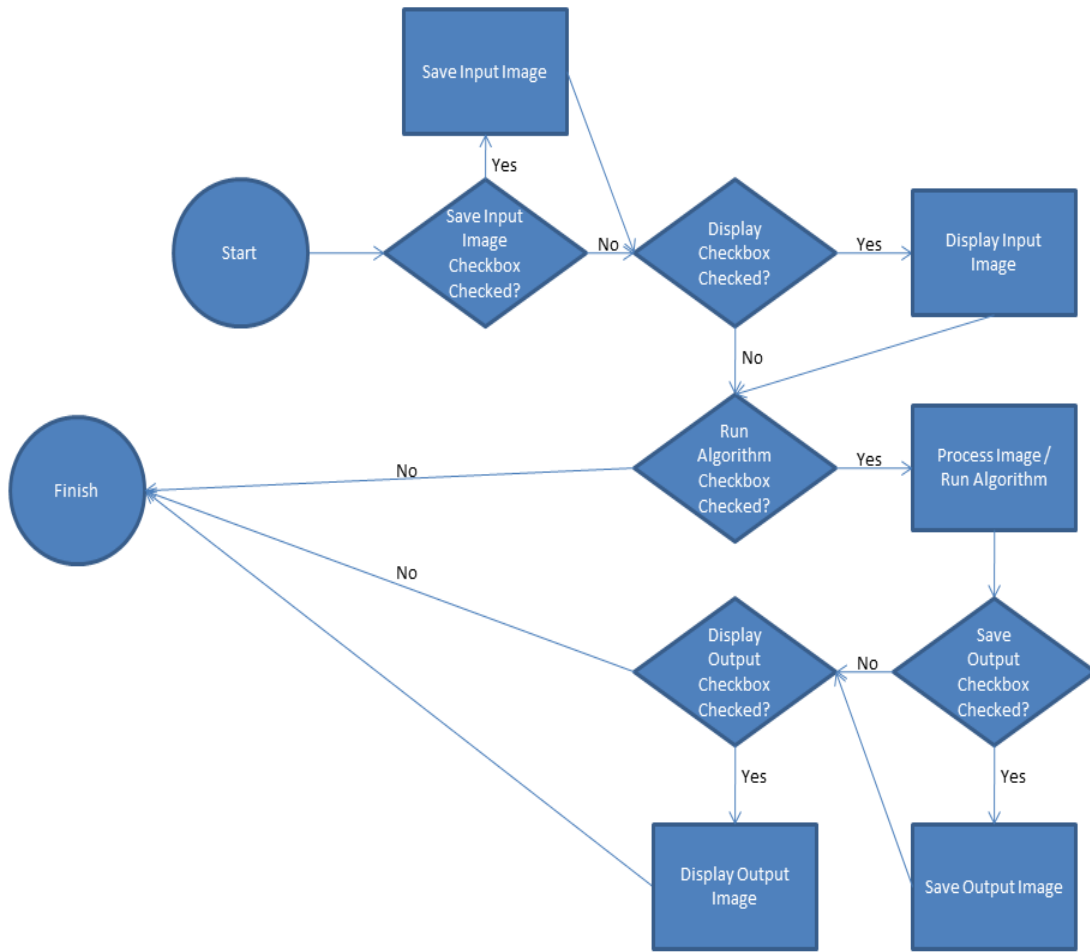


**Figure 43 - DoProcess Function Flowchart**

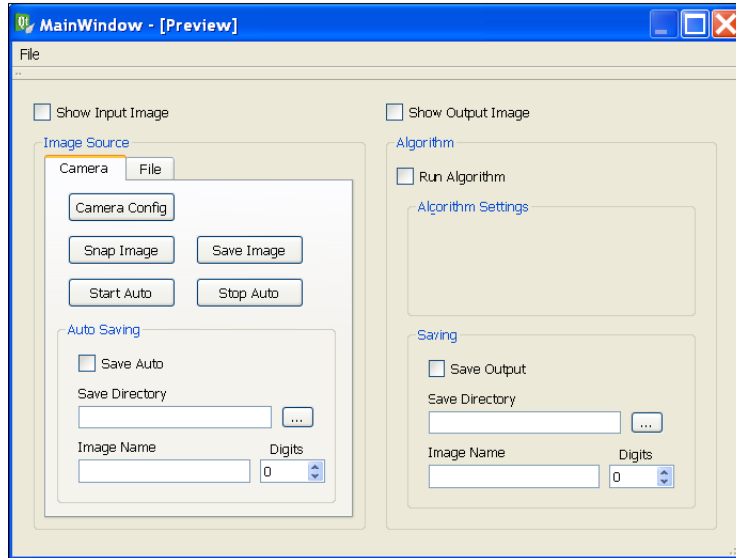


**Figure 44 - Program Dialog with Camera Option**

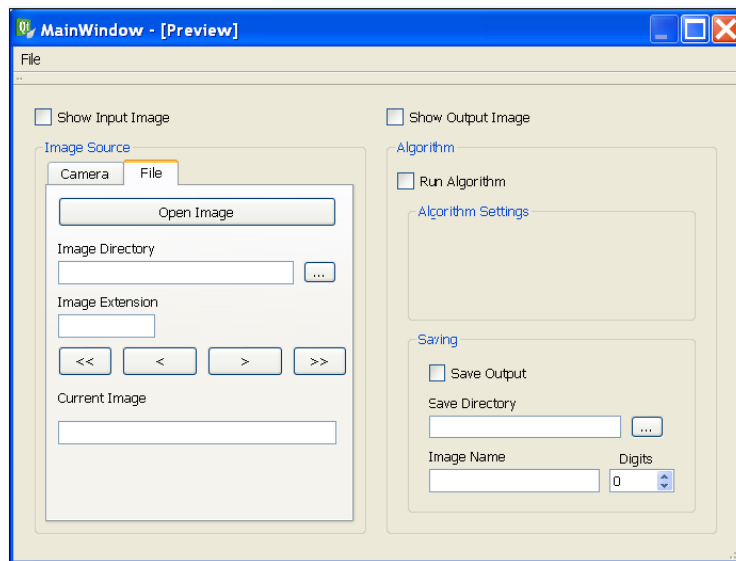


**Figure 45 - Program Dialog with File Loading Option**

### Check Boxes

- Show Input Image – Check box to toggle display for input (raw) image
- Show Output Image – Check box to toggle display of processed image
- Run Algorithm – Check box to enable image processing algorithm
- Save Auto – Checkbox to enable saving all raw images in auto mode



- Save Output – Check box to save output images (single snap and auto mode)

### **Edit Boxes**

- Save Directory – Set location to save files (separate selection for input and output images)
- Image Name (suffix) – Enter an optional suffix to append to save file names
- Current Image – Displays name of current image (for loading files functionality only)
- Digits – Number of digits to use in file name
- Image Directory – Set the directory from which to load images

### **Buttons**

#### **1. Snap Image**

The Snap Image button will snap a single image from the camera and pass the captured image into the function DoProcess(Image).

#### **2. Save Image**

The Save Image button will check if there is a valid image buffer. Upon success, it will open a file save dialog allowing the user to specify a filename and save the image as a .BMP. If there is no valid image buffer, meaning no image has been snapped, a message box will report that there is not a valid image buffer to save.

#### **3. Start Auto**

The Start Auto button will create a timer that will fire once a second (user configurable). Each time the timer fires, the Snap Image functionality will be activated (See Snap Image Button 4.3.1).

#### **4. Stop Auto**

The Stop Auto button will kill the timer spawned in Start Auto (4.3.3). This will stop the system from automatically acquiring images.

#### **5. Camera Configuration**

The Camera Configuration button will spawn a configuration dialog for the related system. In this case, it is a PGR camera dialog. This allows the user to change camera parameters from the HOV Sensing program.

#### **6. Open Image**

The Open Image button will open a single file selection dialog allowing the user to select a .BMP file. Upon success, the file will be loaded and DoProcess(Image) will be called with the loaded image as a parameter.

### **Algorithm Detail**

Details on the algorithms are presented in Appendix III.

# High Occupancy Vehicle People Detection

---

## Background

Detecting and automatically counting vehicle occupants using a visual camera pose numerous challenges such as reflection from the windshield, different operation conditions, and shadows. Most of the work in this regard uses a combination of visual and near infra-red (NIR) range. NIR is almost completely transmitted by the vehicle windshields. Following is a brief description of the state of the art in automatic detection of vehicle occupants.

Dtect provides a commercially available automated system for determining the number of occupants within moving road vehicles (<http://www.vehicleoccupancy.com>.) The system projects two low intensity beams of Infrared (IR) light of different wavelengths onto the vehicle. Two digital photos are taken and merged to produce a single image and then processed by software based algorithms to detect the number of people.

Similarly in (Hao, Chen, Yao, Yang, Bi, & Wang, 2010), the authors use the near infra-red (NIR) illuminator to illuminate the interior of the car and a digital photo is captured using a camera equipped with an NIR filter. This setup reduces the effect of reflection of light from the windshield of the car. The captured photo can be viewed by a human screener or processed by computer vision algorithms to determine the number of occupants. Other work that uses the NIR range is (Wood, Gimmestad, & Roberts, 2003).

Alternate to NIR range is to use thermal imaging systems to detect occupants using their heat map. However the use of athermal metallic coatings on the glass prevents the penetration of these wavelengths through the windshield.

## **Algorithms**

Detecting vehicle occupants poses numerous challenges. We have taken a hierarchical approach to automatically detect people within the vehicles, where at the first level window regions are detected. In the second level only the window regions are searched to detect vehicle occupants.

Based on the results of the background research into the detection algorithms, we decided to look at four approaches for window regions and automated people detection. The approaches chosen for investigation are: Chamfer matching, SIFT (Scale Invariant Feature Transform) based detection, Haar and HOG features based detection. A more detailed explanation of the techniques and their use are presented in the next section.

### **Chamfer Matching Based Window Detection.**

Chamfer matching measures the distance between a template edge map and the edge map of a given input image and uses a sliding window approach to measure distance over whole of the image. The distance between the two edge maps can be effectively computed using a distance transform (Gavrilla, 1998) of the given input image. Each pixel value in the distance transform image is the distance to the closest edge in the

edge map of the input image. Figure 1 shows an input image, its edge map, distance transform (the log of distance transforms is shown for better visualization), and the chamfer matching score using a template of the window region.

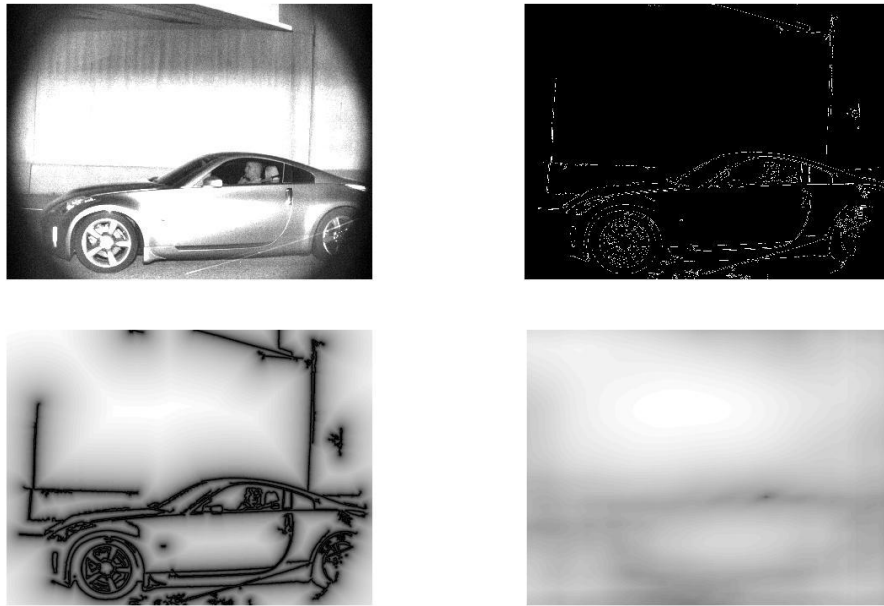


**Figure 1 Input Image, edge map, distance transform and chamfer score.**

To account for different size and shape of the vehicle windows, a variation of the chamfer matching is used. It is explained below.

**a) Generating template contours:**

Instead of using a single edge template, the target object edge map is divided into number of different parts (Jamie, Blake, & Cipolla, 2005). Each part can translate and rotate around its origin, depending upon the variability in shape of the target object. Figure 2 shows the example of template used to detect windows of vehicles, where the template is divided into different line segments.

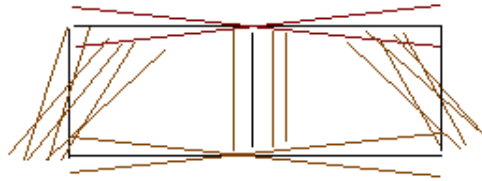


**Figure 2 Example template for window detection.**

**b) Chamfer matching:**

The search window (equal to the size of the template) is moved across the image. At each search location, the distance of each of the line segments to the edge map is computed using the distance transform. From each group of line segments, a line segment is chosen that gives the smallest chamfer score. The chamfer score of the search window is then computed by taking the sum of the chamfer scores of the chosen line segments from each group. The search window that gives the smallest distance is taken as the location of the object in the image.

**Super pixel Segmentation using SIFT**

In the second method we looked at an algorithm that will give us the segmentation of the target objects (window, people) and not just the rectangular boundary. This method comprised of the following steps (Fulkerson, Vedaldi, & Soatto, 2009).

**a) Super pixels segmentation:**

**The image is preprocessed to group similar pixels into super pixels. Mean shift algorithm is used to extract the super pixels from the input image. Examples of input image and its super pixel segmentation are shown in Figure 3. The super pixel segmentation consists of regions that preserve the boundaries in the original image.**

**b) Scale Invariant Feature Transform (SIFT) descriptors extraction:**

**The next step is to extract from each super pixel a feature descriptor. For every  $i$ th pixel in the input image, SIFT features are extracted at a fixed orientation and scale. The extracted descriptors are then quantized using a K-means dictionary (formation of K-means dictionary is explained in the next step). For each super pixel, all the quantized descriptors are aggregated into one L1 normalized histogram. The final descriptor for each super pixel is obtained by**

merging the histograms of  $N$  neighboring super pixels and normalizing the result. Figure 4 shows the location where SIFT features are extracted (not all locations are shown), along with the SIFT descriptors for two of the locations in Figure 4b. Figure 4c shows a super pixel with SIFT features, whose normalized histogram is shown in Figure 4d.

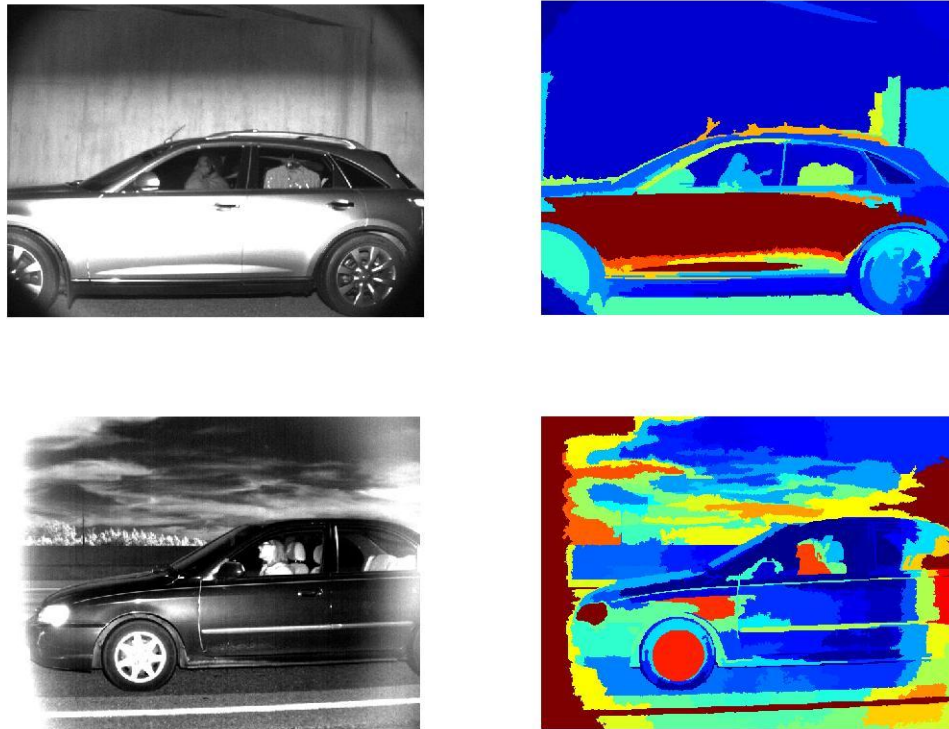


Figure 4 a-d Input images and mean shift based super pixel segmentation.

c) K-means dictionary:

To build a K-means dictionary for quantizing the SIFT descriptors, SIFT descriptors are extracted for each pixel from a set of training images. K-means clustering is performed with  $K=100$ . To build a histogram for a super pixel using this K-means based dictionary, SIFT descriptors within a super pixel are aggregated to the  $K$  bins of the histogram corresponding to the least distance of the descriptor to the cluster centers.

**d) Learning using SVM:**

The positive and negative samples of super pixels are extracting from training images. Descriptor histogram of each super pixel is assigned a 1 or 0 depending upon whether it belongs to the object region or the background. This is then trained using SVM.

During detection phase, histograms of super pixels are extracted and then fed to the SVM, which spits out the class labels.

**e) Refinement using Graph cut:**

Each super pixel is assigned a 1 or 0 by the SVM independently from neighboring super pixels. Graph cut is used to spatially link the neighboring super pixels, which smoothers the resulting segmentation.

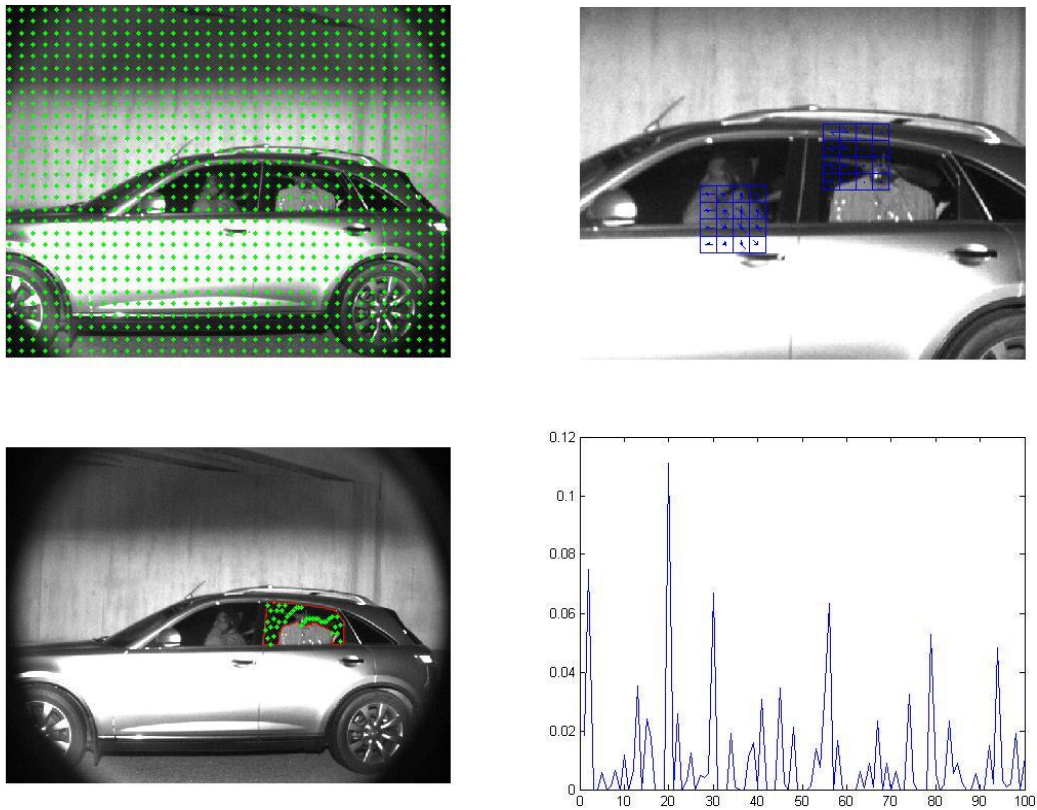


**Figure 5 : First row – location of SIFT features and two SIFT descriptors at two sample locations. Second row – super pixel with SIFT locations and the descriptor histogram for the super pixel.**



## HaarCascade Classifier (Face and Window)

Haar-like features compute the oriented contrasts between regions in the image using simple rectangular features. The rectangular features consist of two sub rectangles: one corresponds to a high interval and the other to low interval. The presence of Haar feature is determined by subtracting the average intensity value of the high region from the low region. If the difference is higher than a threshold value, that feature is present in that region. OpenCV implementation of Haar-like features “HaarCascade classifier” is used for face and window detection (Viola & Jones, 2001).

### a) Training:

**First a set of positive and negative image regions is generated. Positive samples were generated manually from the training images. For negative samples, regions in the image were selected that contained no positive samples. Examples of positive samples of faces and window regions are shown in Figure 5.**



**Figure 6 Examples of positive training samples.**

The locations and the type of Haar features are selected using AdaBoost. Adaboost combines many weak classifiers (Haar features with threshold) to create one strong classifier. The strong classifiers learned using Adaboost are arranged in a cascade in the order of complexity, where each successive

strong classifier is trained using samples that pass through the preceding strong classifiers.

**b) Detection:**

During the detection phase, the search window is moved across the image at multiple scales. At each location, the cascade classifier is evaluated. If at any stage the cascade classifier rejects the region, no further classifiers in the cascade are processed and the search window is moved to the next location. The object is detected in a region if the region is not rejected by any classifier.

**Histogram of Orientated Gradients (HOG).**

This method using dense HOG features (Dalal & Triggs, 2005). The image window is divided into a number of small spatial regions (cells). For each cell a histogram of oriented gradients is computed. For better invariance to illumination changes, the histogram is normalized using larger spatial regions (blocks). The histogram from all the cells are concatenated into one vector called the HOG descriptor of the window region.

**a) Training:**

**First a set of positive and negative image regions is generated. Positive samples were generated manually from the training images. For negative samples, regions in the image were selected that contained no positive samples.** HOG descriptors are computed for all the positive and negative window regions. Binary support vector machine (SVM) is used to distinguish the positive samples from the negative ones.

**b) Detection:**

During the detection phase, the search window is moved across the image. At each location the HOG descriptor is computed for the window region. The HOG descriptor is passed onto the SVM, which classifies the window region into object or background.

## Summary

In addition to the above mentioned methods, some other object detection algorithms were also tested. In light of the performance of different algorithms, we decided to use the HOG features for window detection and the Haar features for vehicle occupant's detection. Below we briefly summarize the advantages and disadvantages of the algorithms tested.

The Chamfer matching based algorithm required no training. However it required a lot of target object edge contours to give a reasonable detection performance. Having a large set of object edge contours affected adversely the speed of the detection algorithm. Moreover, catering for all the different shapes of the windows resulted in a set of edge contours that gave much higher false positive rate. One thing that can be done to improve the performance is to select the edges contours from among all possible contours using Adaboost as is carried out in (Jamie, Blake, & Cipolla, 2005).

The pixel-wise segmentation algorithm using SIFT didn't perform well in all cases. Some of the results are shown in Figure 7, where red contour is the window detected by the algorithm.

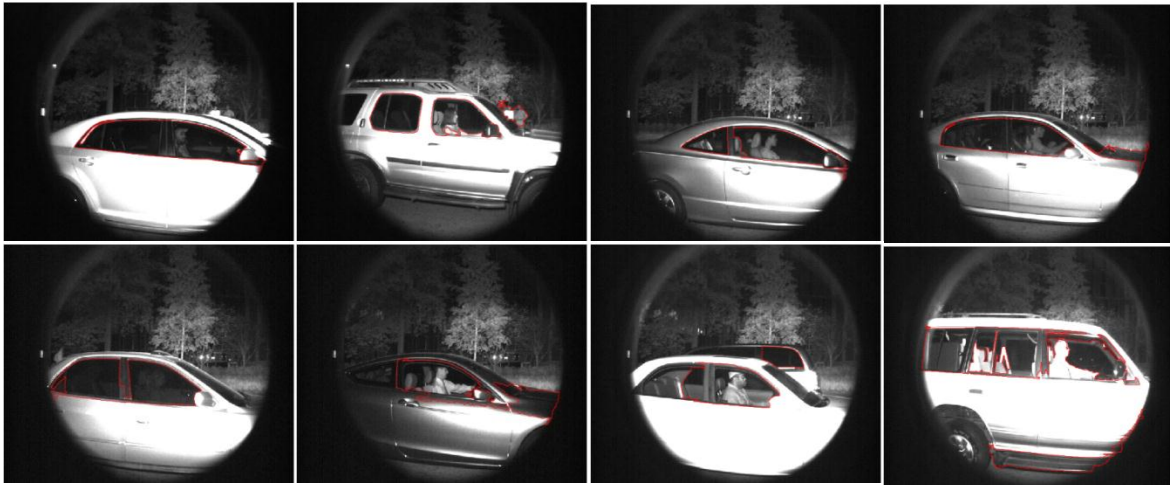


**Figure 7 Window Detection Algorithm.**

Haar features suit detecting faces and facial features and performed reasonable well to detect faces within the window region, where as the HOG features are well suited for objects that have well defined boundaries or silhouettes such as window region.

HaarCascade classifier uses Adaboost to select the optimal features, and it takes from 2-3 days to learn about 15 stages of the HaarCascade. HoG based method uses SVM for learning and the training time is much less (10-20 minutes) as compared to the HaarCascade classifier. However, the HaarCascade can run in real time, whereas the HoG based algorithm runs at about 0.5-1 frames / second.

## **Detection Results**

Based on the results of the preliminary research into the detection algorithms, it was decided to use the HoG based classifier for window detection and HaarCascade classifier for detecting faces. As mentioned above, a hierarchical approach is taken, where at the

first level vehicle window regions are detected using a HoG classifier. In the second level the detected window region is searched for faces using a HaarCascade classifier.

To train the classifiers, training images were taken at different sites. The training images were used to extract the features (HoG for window and Haar-like features for faces), which were then learned/selected using SVM and adaboost respectively. The trained classifiers were then tested on a new set of images taken from a different site.

The test set consisted of 114 images. In six of the images, the laser trigger timing was off a little. As a result, either the back or the front half of the vehicle was captured. For the remaining 108 images, the table below shows the detected, missed and false positive window regions and occupants. For window region the detection rate was 97% and the detection rate for the occupants was 87%.

Window	Detected	105
	Missed	3
	False Positive	5
Occupants	Detected	100
	Missed	15
	False Positive	24

Figure 8 shows some of the detection results. The green rectangle shows the detected window region and the red rectangle shows the detected faces. Please see the Appendix A for more images.



**Figure 8 Detection results**

## **Improvements**

The preliminary detection performance was satisfactory. However there are certain issues that need to be addressed and improved. Such as: in some cases the face detector detects head rest as faces, and occupants partially occluded behind other occupants or window panes are not detected in many cases.

Some of these issues can be addressed by combining the window detection algorithm with a segmentation algorithm. This will result in the extraction of the exact boundary of

the window. The face detector when run within this boundary region should be able to reject many false positives based on where they occur within the window region.

Additionally, if training and testing samples are generated from the same site, the detection performance can be improved considerably. Also, the detection performance can be improved if the imaging device is tuned to give a more uniform image from vehicle to vehicle.

Another issue that needs to be addressed is that the laser did not trigger in a timely manner in about 10% of the vehicles. In some cases it triggered late and in some it did not trigger at all. Mostly these were dark and shiny color vehicles. During the experiments it was noted that if the distance between the laser and the vehicle is more than 15m, the laser captured 100% of the vehicles. At closer distances, about 10% of the vehicles are missed. We think it is due to the use of round (pencil) laser beam. At shorter distances the laser beam is too focused and sometimes may hit the vehicle at an angle where all light is scattered and nothing reflects back. This problem can be alleviated by using a fanned laser module, which forces the beam to diverge in the vertical plane. In the horizontal plane, the laser beam remains collimated. Figure 9 shows a picture of fanned laser module.

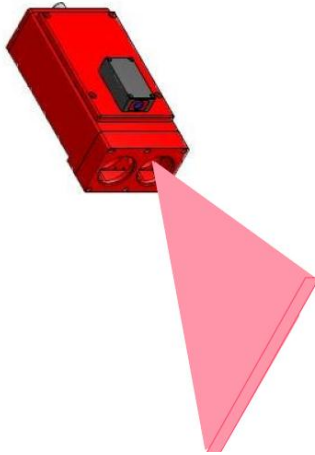


**Figure 9: Fanned laser module (Image taken from <http://www.mdl.co.uk/>)**



## BIBLIOGRAPHY

Dalal, N., & Triggs, B. (2005). Histograms of Oriented Gradients for Human Detection. *Computer Vision and Pattern Recognition*.

Fulkerson, B., Vedaldi, A., & Soatto, S. (2009). Class Segmentation and Object Localization with Superpixel Neighborhoods. *International Conference on Computer Vision*.

Gavrilla, D. (1998). Multi-feature hierarchical template matching using. *ICPR*, (pp. 439-444).

Hao, X., Chen, H., Yao, C., Yang, N., Bi, H., & Wang, C. (2010). A near-infrared imaging method for capturing the interior of a vehicle through windshield. *IEEE Southwest Symposium on Image Analysis and Interpretation*.

<http://www.vehicleoccupancy.com>.

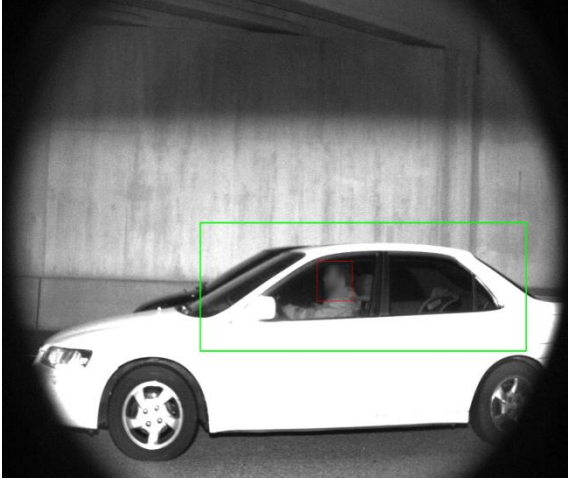
Jamie, S., Blake, A., & Cipolla, R. (2005). Contour-Based Learning for Object Detection. *International conference on computer vision*.

Viola, P., & Jones, M. (2001). Rapid object detection using a boosted cascade of simple features. *Computer Vision and Pattern Recognition*.

Wood, J., Gimmestad, G., & Roberts, D. (2003). Covert camera for screening of vehicle interiors and hov enforcement. *SPIE-The international Society for optical Engineering*.

Appendix A







## Appendix IV: LED Evaluation

### Assessing Power Requirements for Prototype LED Board

To measure the current travelling through a string of LED I measured the voltage across a 2 Ohm resistor in an LED string using the Fluke 192B Scopemeter (battery powered oscilloscope). The battery powered oscilloscope must be used on these boards because of the way the strobe circuit is built. The LED board's "+" is wired to VCC while its "-" is connected to a transistor that provides a path to ground when the transistor is activated. If an oscilloscope that shares an earth ground with the power supply is used, the LEDs will be on simply by being connected to the oscilloscope (having a path to ground) and will burn out in a matter of seconds (meant to be strobed at only 100-150 microseconds at 1 amp). The Fluke measured roughly 2 volts (see image below) over the 150 microseconds the LEDs were on. Using Ohms Law ( $V = IR$ ), we can calculate the amperage ( $I = V \ / \ R$ ).  $I = 2 \ / \ 2 = 1$  amp. A voltage of 29 volts was used to drive the LEDs for this test. One board consisting of 14 strings of LEDs require 14 amps at 29 volts to maximize light output while not burning itself out.

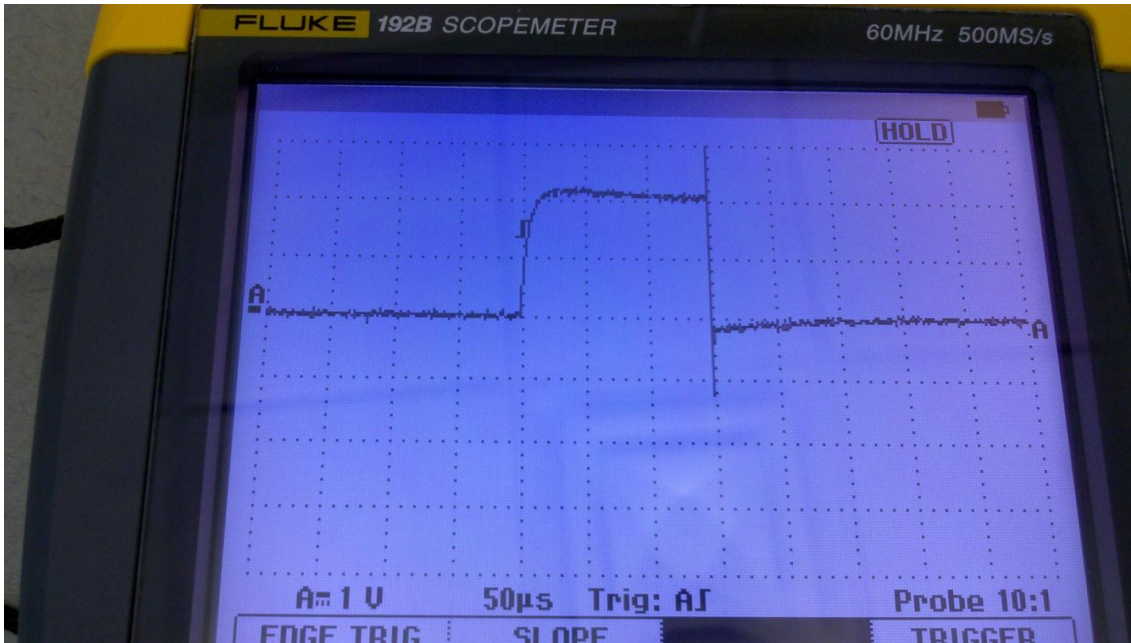
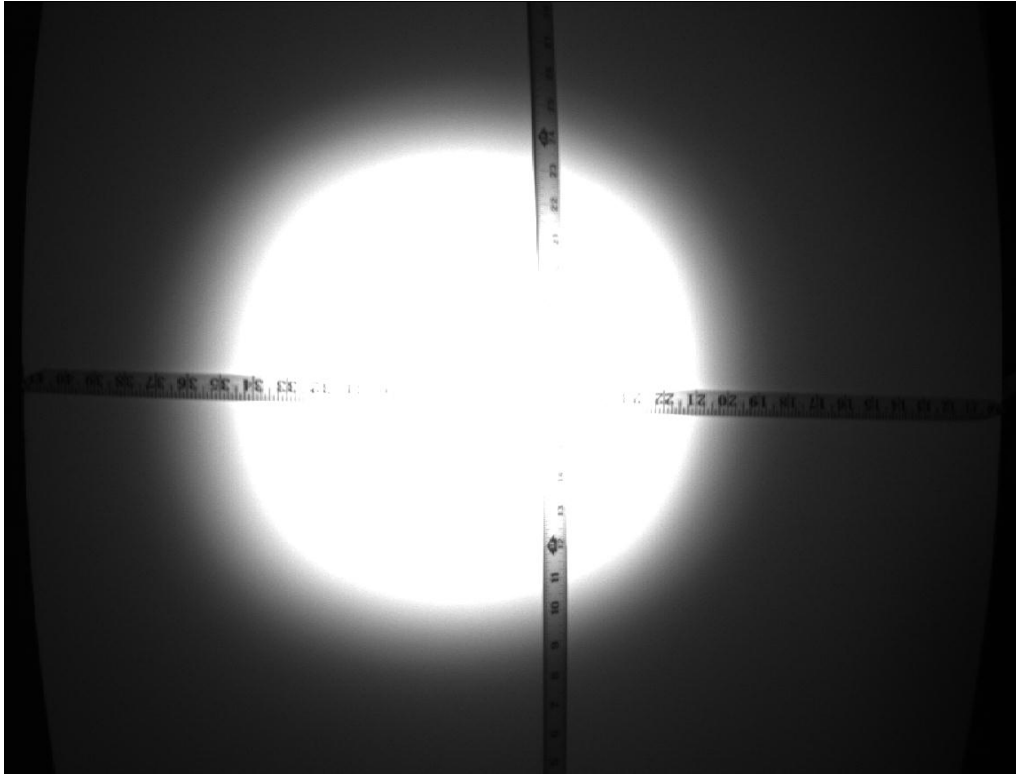


Figure 47: Voltage measured across LED array when pulsed

### Assessing Light Output of Prototype LED Board

First, the horizontal and vertical output angles of the prototype LED board were calculated. The image below shows how the measurements were taken. There are two sets of angles corresponding to the “inner brighter” circle and the “outer faded” circle. The outer circle measured from 18 to 37.5 inches, for a 19.5 inch width. It measured 8 to 26 inches for an 18 inch height. The photograph was taken from 2 feet away. The “cone of light” output is 39.093 degrees horizontally and 36.869 degrees vertically. The inner circle had a 14 inch width and a 13.5 inch height for a 30.25 degree horizontal angle and a 29.35 degree vertical angle. Camera settings are unknown for this picture.



**Figure 48: Measuring cone of light from LED array**



**Figure 49: Cropped region used for LED tests**

The second test to characterize the light source. The picture above was taken with a .94 ms integration (and strobe) time with 0.0 gain on the grey target. The distance was approximately 26 inches and the light seemed to fit on the surface nicely. The image was cropped to the region outlined in the above image.

The next two images show the cropped regions using a color map followed by contours of the color map. To take this picture the camera was mounted to the table. The same grey target from the previous test was placed roughly two feet from the camera. The LED array was held below to the camera aiming at the board as perpendicular as possible (eyeballing). Multiple pictures were taken until the light was completely on the board. The two images were generated in Matlab 7.5.0 (2007b) from the cropped image above.



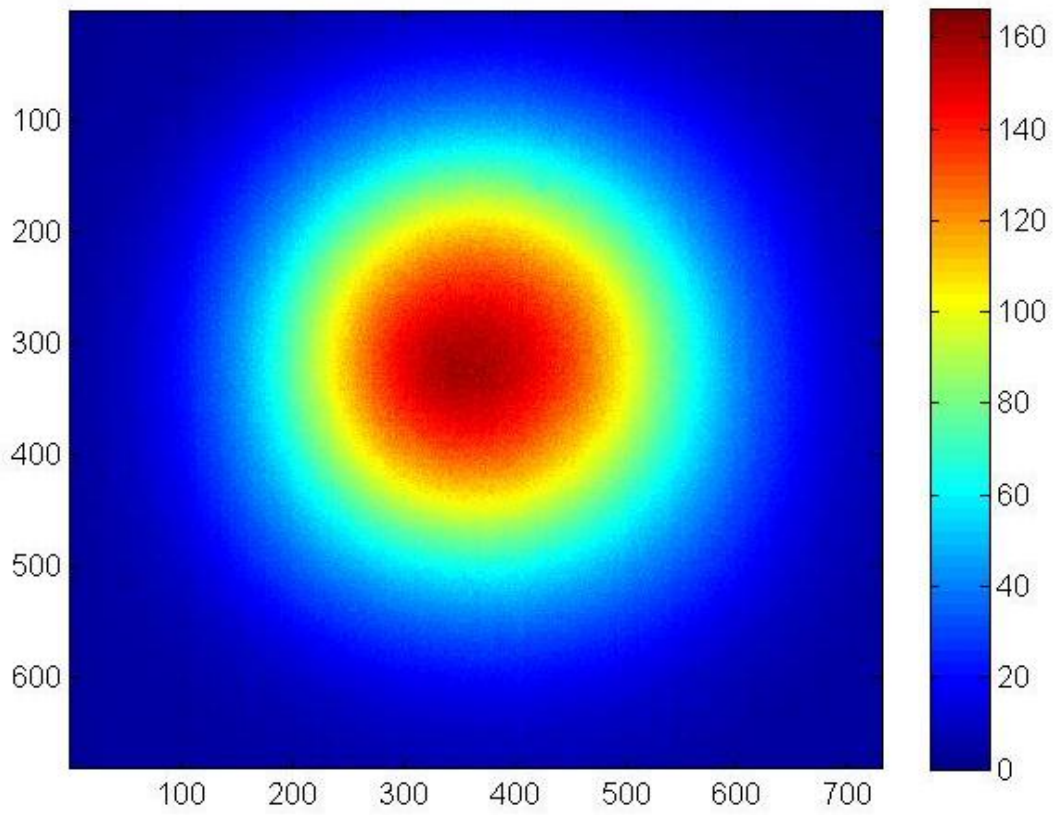


**Figure 50 Colormap of intensity values for LED array**

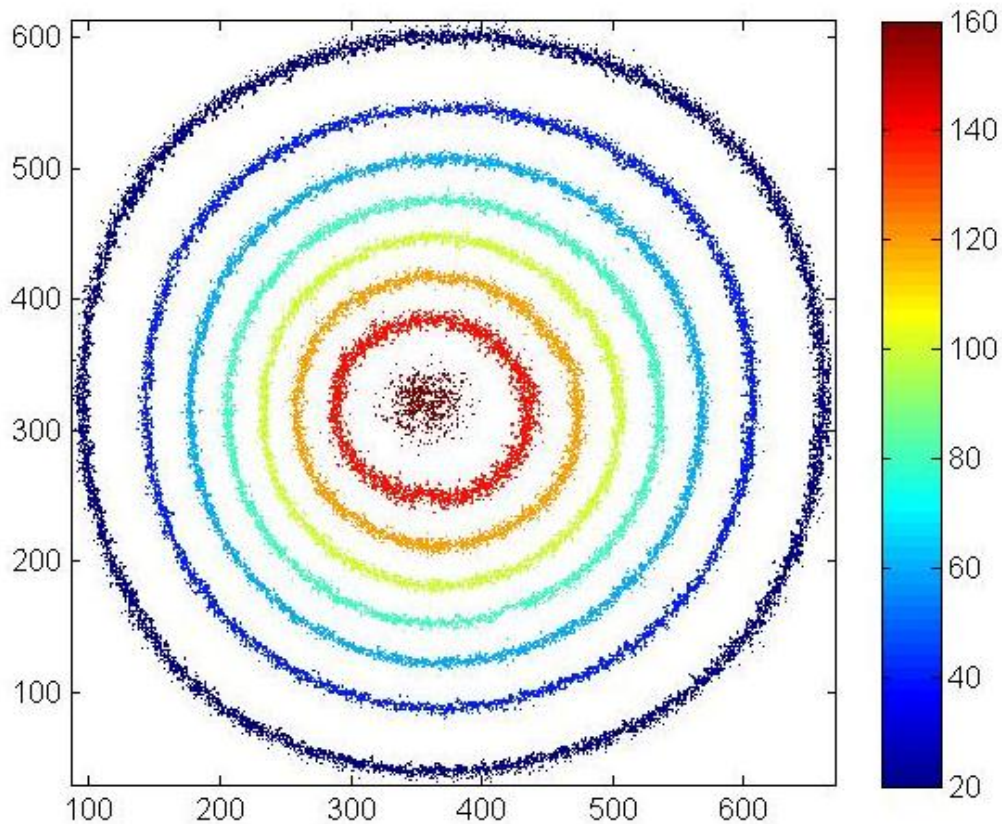


**Figure 51: Contours of colormap for LED array**

### **Comparing Prototype LED Board with MVS-5770F-01**

For this experiment the THORLABS PDA520 light meter and Tektronix TDS 2042B oscilloscope were used and set up in the following manner (image below). Thor Lab's neutral density (ND) filters were placed in front of the light meter until a non-saturated reading was taken. The test was done for the led array and the MVS-5770F-01 and the results are shown on the following graphs.

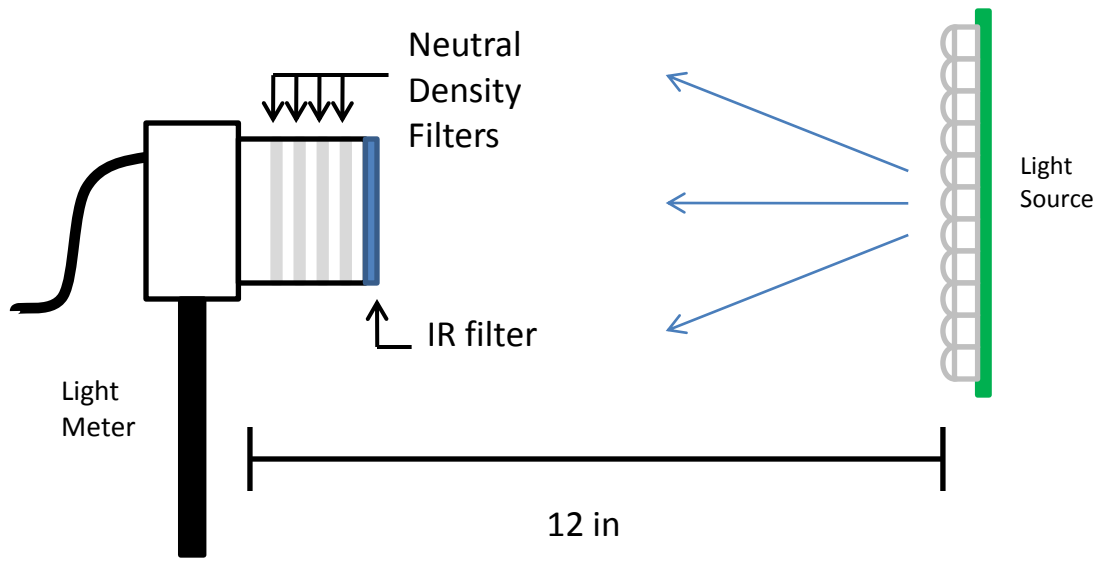
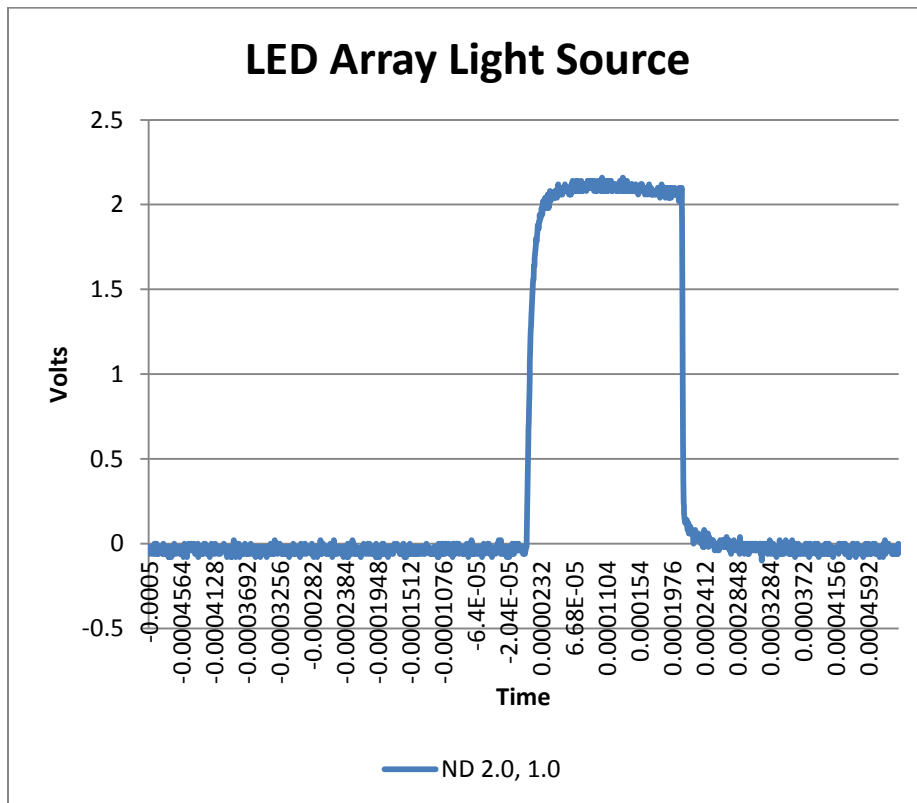
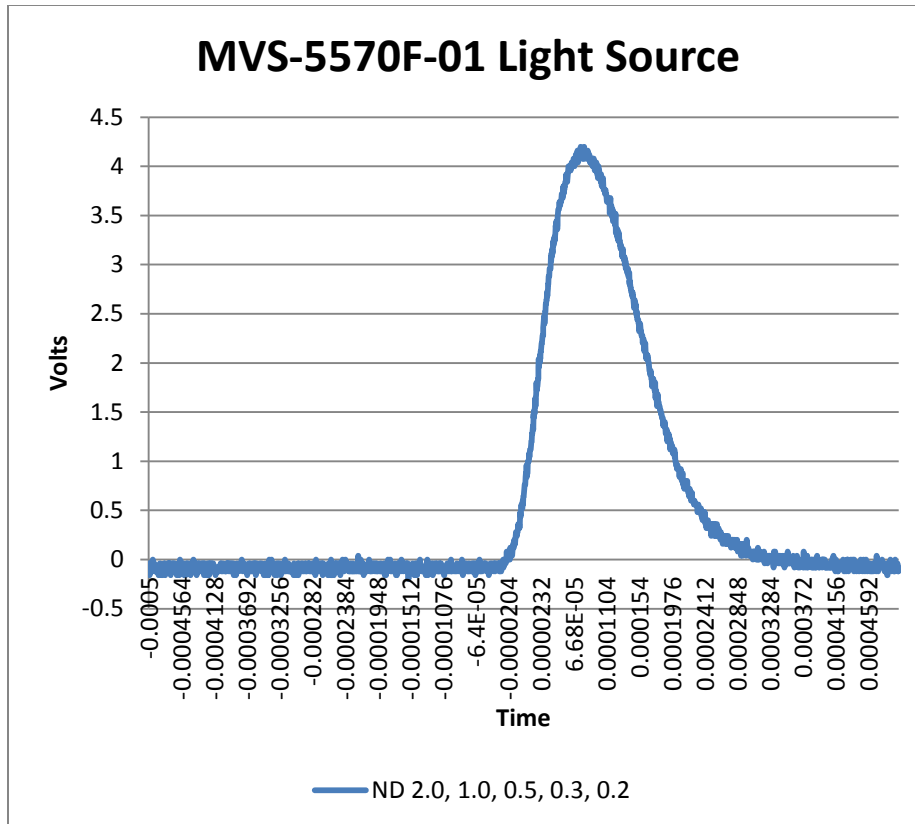


Figure 52: Experiment Setup





The areas under the graphs during the pulses are 0.000611 for the MVS-5770F and 0.000422 for the LED array. The filters used were 2.0, 1.0, 0.5, 0.3, 0.2 for the MVS-5770 and 2.0, 1.0 for the LED array.

The power for the MVS-5770F would be  $0.000611 * 10^2 * 10^1 * 10^{.5} * 10^{.3} * 10^{.2} = .000611 * 100 * 10 * 3.1622 * 1.999 * 1.585 = 6.122$

The power for the LED array would be  $0.000422 * 10^2 * 10^1 = .422$

Per unit area, the MVS-5770F is roughly  $6.122 / .422$  or 14.507 times stronger (where the area is the surface area of the light meter.)

Now we need to take account the area projected by the light sources. I will use 10 feet as the distance (math easier).

The MVS-5770F outputs a rectangular pattern of 75 by 25 degrees. At 10 feet, it would project a 15.347 by 4.434 foot rectangle for a 68.047 foot area.

The LED array outputs a 30.25 by 29.35 degree oval. At 10 feet, it would project a 5.406 by 5.238 oval. I will just approximate to a 5.3 foot circle to get a 22.061 area.

The MVS-5770F has an output area of roughly  $68.047 / 22.061$  or 3.084 times larger.

If we multiply the light output by area scaling factors,  $14.507 * 3.084$ , we get 44.747 or the number of LED arrays that equal one MVS-5770F. If it takes 44.747 led arrays of 9 by 14 LEDs or 126 total LEDs, roughly 5638 LEDs are need just to match the output power of the strobe.